Radiation Report
SLVK045–February 2020

Single-Event Effects Test Report of the TPS7H1101A-SP LDO

ABSTRACT

The purpose of this study is to characterize the single-event-effect (SEE) performance due to heavy-ion irradiation of the TPS7H1101A-SP. Heavy-ions with LET_{EFF} ranging from 48 to 85 MeV·cm^2/mg were used to irradiate production RHA devices in 31 experiments with fluences ranging from 10^6 to 5 x 10^7 per run. The results demonstrated that the TPS7H1101A-SP is SEL-free up to 85 MeV·cm^2/mg at T = 125°C, SEB/SEGR/SEFI-free up to 85 MeV·cm^2/mg at room temperature, and across the full electrical specifications. The SET cross section is presented, discussed, and shown to have a nearly free on orbit upset rate.

Contents

List of Figures

List of Tables

Trademarks

Kevlar is a registered trademark of E.I. du Pont de Nemours and Company.
LabVIEW is a registered trademark of National Instruments.
All other trademarks are the property of their respective owners.

1 Introduction

The TPS7H1101A-SP is a space-grade, radiation-hardened, 1.5-V to 7-V input, 3-A, Linear Low Dropout (LDO) regulator. The device contains a P-channel MOSFET as the pass element. The device supports a maximum of 3 A of continuous current, however, two devices can be parallel to service up to 6 A of load. The device has an excellent Power Supply Rejection Ratio (PSRR) and noise performance, making it an ideal choice in any step-down clean power supply requirement. The follow are some of the device features:

- Programmable Current Limit (PCL)
- Current Sense (CS) pin for health monitoring
- Soft-Start (SS) pin for programable start-up and down slew rate control
- Power Good (PG) open-drain pin for health monitoring and power sequencing
- Programmable current foldback limit

The device is offered in a thermally-enhanced 16-pin ceramic, dual in-lineflat package. Table 1 lists the general device information and test conditions. Visit the TPS7H1101A-SP product page for more detailed technical specifications, user's guides, and applications notes.

Table 1. Overview Information(1)

DESCRIPTION	DEVICE INFORMATION
TI Part Number	TPS7H1101A-SP
Orderable Name	5962R1320202VXC
Device Function	Linear Low Dropout (LDO) regulator
Technology	250 nm Linear Bi-CMOS
Exposure Facility	Radiation Effects Facility, Cyclotron Institute, Texas A&M University
Irradiation Temperature	25°C and 125°C (For SEL Testing)

(1) TI may provide technical, applications or design advice, quality characterization, and reliability data or service. Providing these items shall not expand or otherwise affect TI's warranties as set forth in the Texas Instruments Incorporated Standard Terms and Conditions of Sale for Semiconductor Products and no obligation or liability shall arise from Semiconductor Products and no obligation or liability shall arise from TI's provision of such items.

2 Single-Event Effects

The primary concern for the TPS7H1101A-SP is the robustness against the destructive single event effects (DSEE): single event latch-up (SEL), single event burn-out (SEB), and single event gate rupture (SEGR). In mixed technologies such as the BiCMOS process used on the TPS7H1101A-SP, the CMOS circuitry introduces a potential for SEL susceptibility.

SEL can occur if excess current injection caused by the passage of an energetic ion is high enough to trigger the formation of a parasitic cross-coupled PNP and NPN bipolar structure (formed between the p-substrate and n-well and n+ and p+ contacts) [1, 2]. If formed, the parasitic bipolar structure creates a high-conductance path (creating a steady-state current that is orders-of-magnitude higher than the normal operating current) between the power and ground that persists (is “latched”) until power is removed or until the device is destroyed by the high-current state. The design and process techniques used on the TPS7H1101A-SP for SEL-mitigation were sufficient as the TPS7H1101A-SP exhibited no SEL events with heavy-ions of up to LET_{EFF} = 85 MeV·cm^2/mg at a flux of 10^5 ions/cm^2·s, fluences in excess of 10^7 ions/cm^2, and a die temperature of 125°C.

Since this device is designed to conduct large currents (up to 3 A) and withstand up to 7 V during the off-state, the LDMOS (P-type, pass element) introduces a potential susceptibility for SEB and SEGR [3, 4]. The TPS7H1101A-SP was evaluated for these destructive effects under both possible cases (enabled and disabled) at die temperatures of 25°C (when disabled, I_{LOAD} = 0 A and (V_{IN} - V_{OUT}) = 5.2 V) and 34°C (when enabled, I_{LOAD} = 3 A and (V_{IN} - V_{OUT}) = 2 V). It has been shown that the SEB susceptibility decrements with elevated temperatures [5] and for that reason, this test was conducted near room temperature. During the SEB/SEGR testing, not a single current event was observed, demonstrating that the TPS7H1101A-SP is SEB/SEGR-free up to LET_{EFF} = 85 MeV·cm^2/mg at a flux of 10^5 ions/cm^2·s, fluences in excess of 10^7 ions/cm^2, and a die temperature of 25°C to 34°C.

The TPS7H1101A-SP shows two different single event transients (SET) signatures under heavy-ion irradiation. Both of these SET were self-recoverable, without the need of external intervention. The signature with the highest likelihood of observation is a fast transient on the output voltage. This upset has a typical transient time of 1.2 µs, and shows onset near LET_{EFF} = 45 MeV·cm^2/mg and a cross section of 8 x 10^{-6} cm^2/device for an upset greater than ±5% than the nominal voltage (at V_{OUT} = 1.2 V). The second observed signature is a slow transient on the output voltage. During this upset, the soft-start capacitor is discharged and a full re-start cycle is initiated. The recovery time is dominated by the soft-start capacitor during this type of SET. This type of transient was just observed once at LET_{EFF} = 85 MeV·cm^2/mg. For more details on the SET results, see Section 8.

3 Test Device and Evaluation Board Information

The TPS7H1101A-SP is packaged in a 16-pin, thermally-enhanced, dual-ceramic, flat pack package (HKH) as shown in Figure 1. The TPS7H1101SPEVM evaluation board was used to evaluate the performance and characteristics of the TPS7H1101A-SP under heavy-ions. Figure 2 shows the top views of the evaluation board used for the radiation testing. Figure 3 shows the board schematics for the EVM used for the heavy-ion testing campaign. Table 2 shows the values used for the R27 and R28 to adjust the output voltages for the testing. See the TPS7H1101A-SP Evaluation Module for more information about the evaluation board.

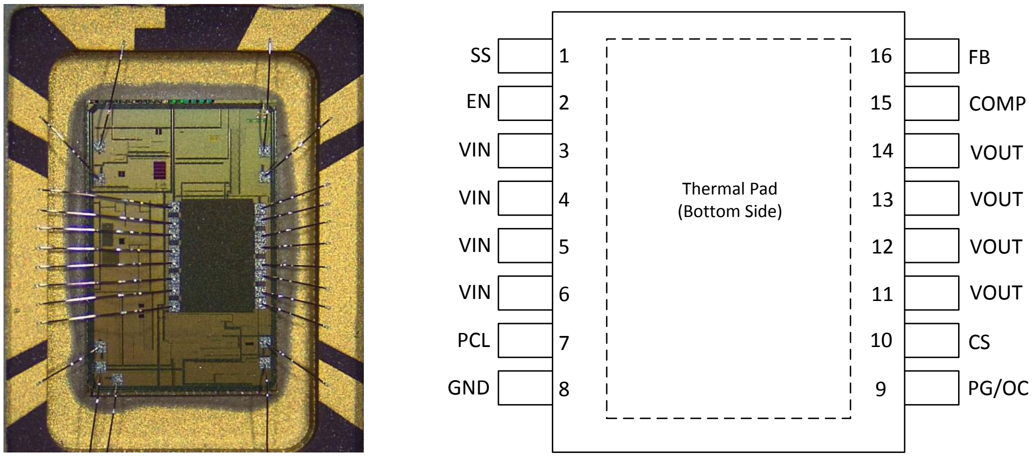

The package lid was removed to reveal the die face for all heavy ions testing.

Figure 1. Photograph of Delidded TPS7H1101A-SP [Left] and Pin Out Diagram [Right]

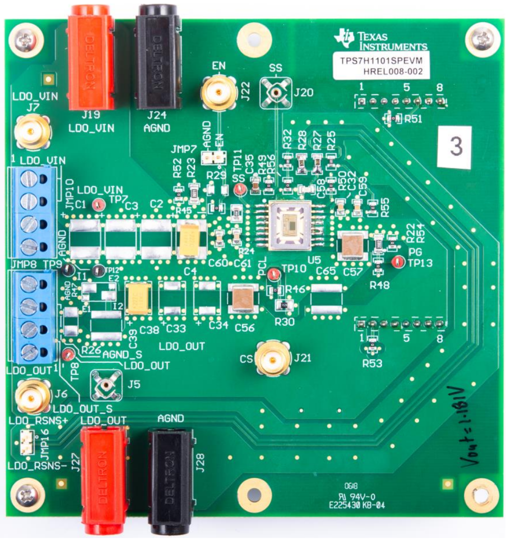

Figure 2. TPS7H1101A-SP Board Top View

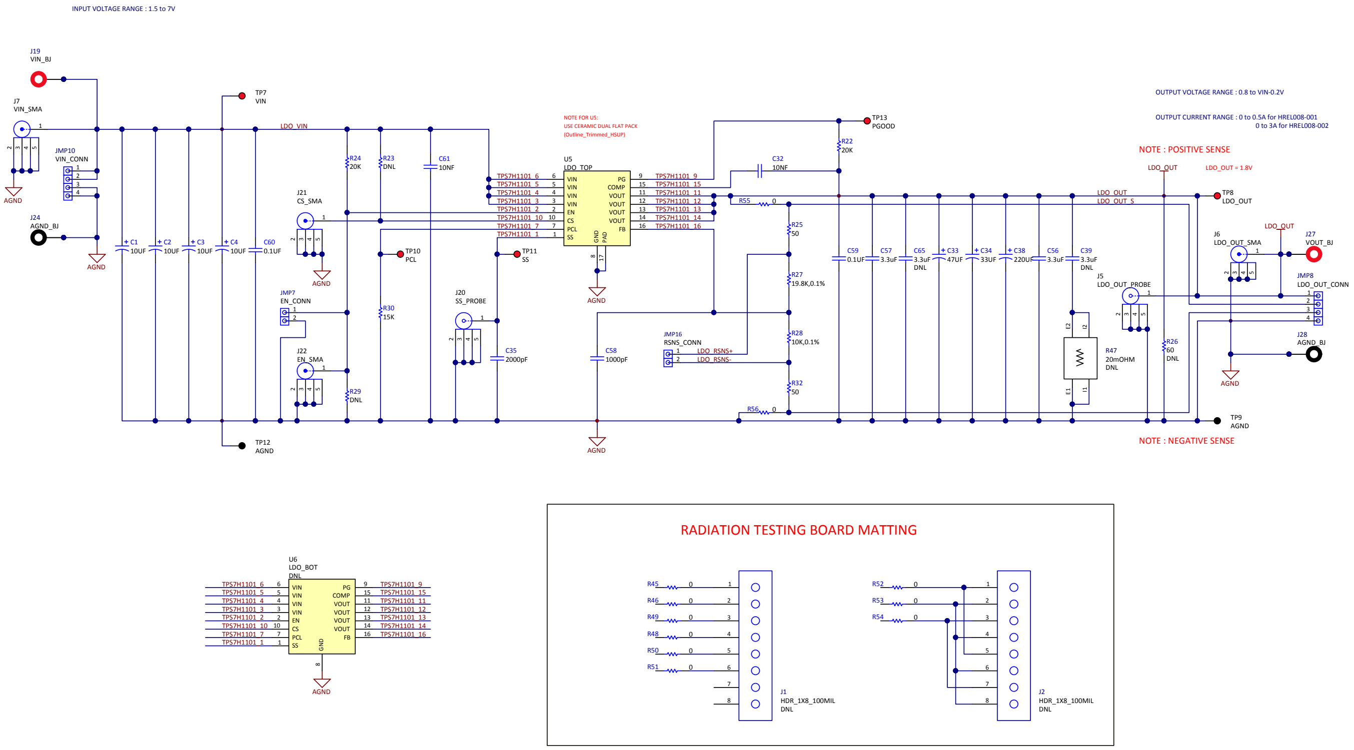

R27 and R28 were adjusted per Table 2.

Figure 3. Schematics of the TPS7H1101 EVM Used for the Heavy-ion Testing

Table 2. R27 and R28 Values per Output Voltage

R27 (KΩ)	R28 (KΩ)	V_{OUT} (V)
16.2	2.21	4.94
32.4	16.2	1.8
11.8	12.4	1.18
37.4	12.1	2.46

4 Irradiation Facility and Setup

The heavy-ion species used for the SEE studies on this product were provided and delivered by the TAMU Cyclotron Radiation Effects Facility [6] using a superconducting cyclotron and an advanced electron cyclotron resonance (ECR) ion source. At the fluxes used, ion beams had good flux stability and high irradiation uniformity over a one inch diameter circular cross sectional area for the in-air station. Uniformity is achieved by magnetic defocusing. The flux of the beam is regulated over a broad range spanning several orders of magnitude. For the bulk of these studies, ion flux of 10^4 and 10^5 ions/cm^2·s were used to provide heavy-ion fluences of 10^6 and 10^7 ions/cm^2.

For the experiments conducted on this report, ^{63}Cu ions at angle of 50º of incidence were used for an LET$_{EFF}$ of 35 MeV·cm^2/mg. ^{109}Ag ions at angles of 0º and 32º of incidence were used for an LET$_{EFF}$ of 48.5 and 57 MeV·cm^2/mg, respectively. Also, ^{141}Pr ions at angles of 0º and 38.8º of incidence were used for an LET$_{EFF}$ of 61 and 85 MeV·cm^2/mg, respectively. The total kinetic energy of ^{63}Cu, ^{109}Ag, and ^{141}Pr in vacuum are 0.944, 1.63, and 2.11 GeV, respectively. Ion uniformity for these experiments was between 92% and 98%.

Figure 4 shows the TPS7H1101A-SP test board used for the experiments at the TAMU facility. Although not visible in this photo, the beam port has a 1-mil Aramica window to allow in-air testing while maintaining the vacuum within the accelerator with only minor ion energy loss. Test points were soldered on the back for easy access of the signals while having enough room to change the angle of incidence and maintaining the 40 mm distance to the die. The in air gap between the device and the ion beam port window was maintained at 40 mm for all runs.

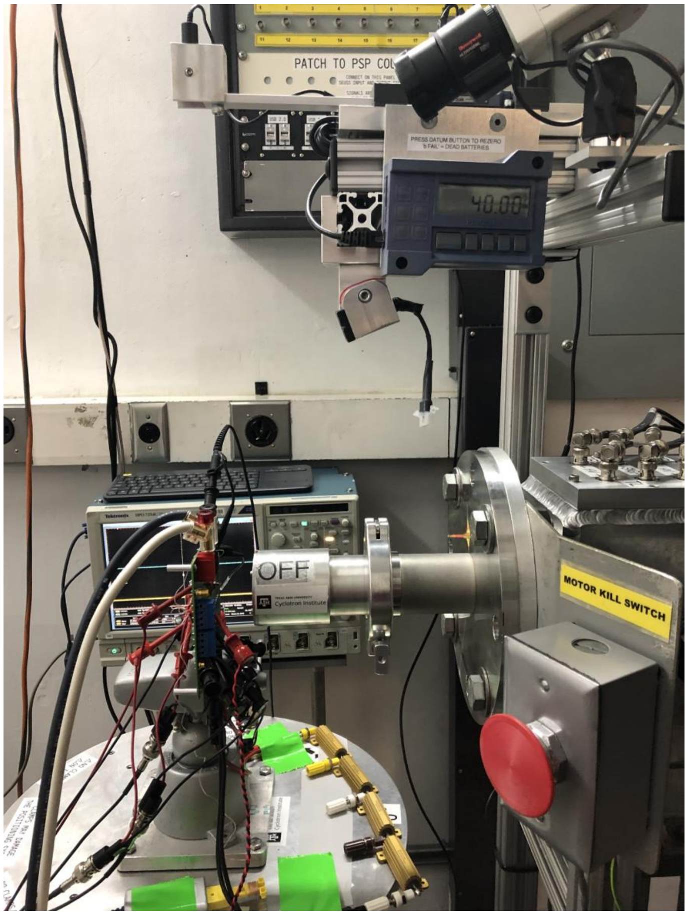

Figure 4. Photograph of the TPS7H1101A-SP Mounted on the TPS7H1101A EVM in Front of the Heavy Ion Beam Exit Port at the TAMU Accelerator Facility

5 Depth, Range, and LET$_{EFF}$ Calculation

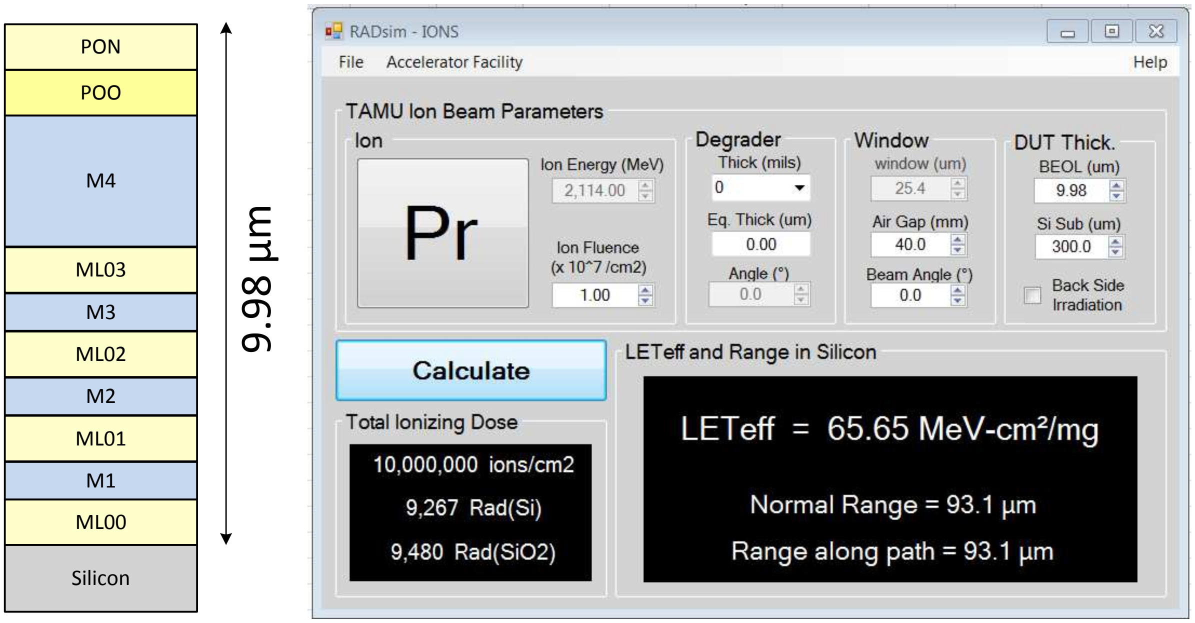

TAMU Ion Beam Parameters

Ion: Pr

Ion Energy (MeV): 2,114.00

Ion Fluence (x 10^7 /cm2): 1.00

Degrader Thick (mils): 0

Eq. Thick (um): 0.00

Angle (°): 0.0

Window window (um): 25.4

Air Gap (mm): 40.0

Beam Angle (°): 0.0

DUT Thick. BEOL (um): 9.98

Si Sub (um): 300.0

☐ Back Side Irradiation

Total Ionizing Dose

10,000,000 ions/cm2

9,267 Rad(Si)

9,480 Rad(SiO2)

LETeff and Range in Silicon

LETeff = 65.65 MeV-cm²/mg

Normal Range = 93.1 µm

Range along path = 93.1 µm

Figure 5. Generalized Cross section (Left) of the LBC7 Technology BEOL Stack on the TPS7H1101A-SP. GUI of RADsim Application (Right) Used to Determine Key Ion Parameters

The TPS7H1101A-SP is fabricated in the TI Linear BiCMOS 250-nm process with a back-end-of-line (BEOL) stack consisting of three levels of standard thickness aluminum metal on a 0.6-µm pitch and a fourth level of thick aluminum. The total stack height from the surface of the passivation to the silicon surface is 9.98 µm based on nominal layer thickness as shown in Figure 5. No polyimide or other coating was present, so the uppermost layer was the nitride passivation layer (PON). Accounting for energy loss through the 1-mil thick Aramica (Kevlar®) beam port window, the 40-mm air gap, and the BEOL stack over the TPS7H1101A- SP, the effective LET (LET$_{EFF}$) at the surface of the silicon substrate and the depth and ion range was determined with the custom RADsim-IONS application (developed at Texas Instruments and based on the latest SRIM2013 [7] models). Table 3 shows the results. The stack was modeled as a homogeneous layer of silicon dioxide (valid since SiO_2 and aluminum density is similar).

Table 3. Copper, Silver, and Praseodymium Ion LET$_{EFF}$, Depth, and Range in Silicon

ION TYPE	ANGLE OF INCIDENCE (°)	DEPTH OF SILICON (µm)	RANGE OF SILICON (µm)	LET$_{EFF}$ (MeV·cm^2 /mg)
^{63}Cu	50	69.1	107.5	32.63
^{109}Ag	0	87.8	87.8	48.46
^{109}Ag	32	72.9	86	57.62
^{141}Pr	0	93.1	93.1	65.65
^{141}Pr	38.8	70.3	90.2	84.98

6 Test Setup and Procedures

SEE testing was performed on a TPS7H1101A-SP device mounted on a TPS7H1101SPEVM. The device power was provided by using the J19 (V$_{IN}$) and J24 (GND) banana inputs using the N6702 precision power supply in a 4-wire configuration. Channel #2 and #3 (model: N6776A) were paralleled and the current clamp was set up to 4 Amps during all the testing. Discrete power resistors were used to load the device to 0.5 (SET) and 3 Amps (SET, SEB/SEGR).

For the SEL, SEB, and SEGR, the device was powered up to the maximum recommended operating voltage of 7 V and loaded with the maximum load of 3 A. The output voltage was set to 5 V for SEL and 5 V and 1.8 V for the SEB/SEGR testing. For the SEB/SEGR characterization, the device was tested under enabled and disabled modes. The device was disabled by using the JMP 7, connecting EN to GND. The discrete load resistor was connected, even when the device was disabled, to help differentiate if an SET momentarily activated the device under the heavy-ion irradiation. **Not a single current increment event was observed during any of the SEL, SEB/SEGR testing.**

For the SET characterization, the device was powered up to 5 V for the 2.5-V Vout case, and 1.8 V for the 1.2-V case.

The SET events were monitored using two National Instruments (NI) PXie 5105 (60 MS/s and 60 MHz of bandwidth) digitizer modules and one Tektronix DPO7104C Digital Phosphor Oscilloscope (DPO) with four channels of 40 GS/s and 2.5 GHz of bandwidth. The DPO was used to monitor the soft start (SS) and V_{OUT} signals, and was triggered from the SS using a negative edge trigger. The first NI-PXIe Scope card (#1) was used to monitor the following:

- V_{OUT}
- V_{IN}
- CS
- PG
- EN
- PCL

They were triggered from V_{OUT} using a window trigger set at 3% around the nominal output voltage. The second NI-PXIe Scope card (#2) was used to monitor PG and V_{OUT} and was triggered from PG using an edge negative trigger. With the exception of the DPO digital oscilloscope, all equipment was controlled and monitored using a custom-developed LabVIEW® program (PXI-RadTest) running on a NI-PXIe-8135 Controller. Figure 6 shows a block diagram of the setup used for SEE testing on the TPS50601-SP. Table 4 shows the connections, limits, and compliance values that were used. In general, the TPS7H1101A-SP was tested at room temperature (no external heating applied). A die temperature of 125°C was used for SEL testing and was achieved by attaching three parallel power resistors (model: RP60800R0100JNBK) to the thermal pad on the back of the board using solder paste. The die temperature was monitored during the testing using a K-Type thermocouple attached to the heat slug of the package and correlated using a thermal camera before the SEE characterization since the values were not exactly the same and offset compensation was used. Figure 7 shows an image where the die and thermocouple reading are shown at the same time. During SEB testing, the device was chilled by using a vortex tube aimed at the die since SEB is worst case at low temperature. This was used only when the device was enabled and loaded to 3 Amps.

Table 4. Equipment Set and Parameters Used for the SEE Testing the TPS7H1101A-SP

PIN NAME	EQUIPMENT USED	CAPABILITY	COMPLIANCE	RANGE OF VALUES USED
V_{IN}	Agilen N6700 PS (Channel #2 and 3 in Parallel)	6 A	4 A	1.8, 5, and 7 V
Oscilloscope Card	NI-PXIe 5105	60 MS/s	-	20 MS/s
Digital Oscilloscope	Tektronix DPO7104C	40GS/s	-	20MS/s
Digital I/O	NI-PXIe 6556	200 MHz	-	50 MHz

All boards used for SEE testing were fully checked for functionality. Dry runs were also performed to ensure that the test system was stable under all bias and load conditions prior to being taken to the TAMU facility. During the heavy-ion testing, the LabView control program powered up the TPS7H1101A-SP device and set the external sourcing and monitoring functions of the external equipment. After functionality and stability had been confirmed, the beam shutter was opened to expose the device to the heavy-ion beam. The shutter remained open until the target fluence was achieved (determined by external detectors and counters). During irradiation, the PXIe-5101 scope cards continuously monitored the signals. When the output voltage exceeds the pre-defined 3% window trigger, or when the PG signal changed from High to Low (using a negative edge trigger), a data capture was initiated on the scope cards. 20 k samples were recorded with a pre-defined 20% reference (percent of the data vector before the trigger happen).

The NI scope cards captured events lasting up to 1 ms (20 k samples at 20 MS/s). In parallel, the DPO monitored SS and V_{OUT} triggering from SS using a negative edge trigger. The sample rate was set to 20 MS/s with a much longer time capture window of 10 ms total (1 ms/div) and recording 20% or (2 ms) before the event. The DPO was set to fast frame during the test. Under this configuration, the scope has a 3.2-µs update rate, indicating that it can re-arm and be ready for next trigger within 3.2 µs. In addition to monitoring the voltage levels of the two scopes and one DPO, V_{IN} current and the +5 V signal from TAMU were monitored at all times. No sudden increases in current were observed (outside of normal fluctuations) on any of the test runs indicated that no SEL events occurred during any of the tests.

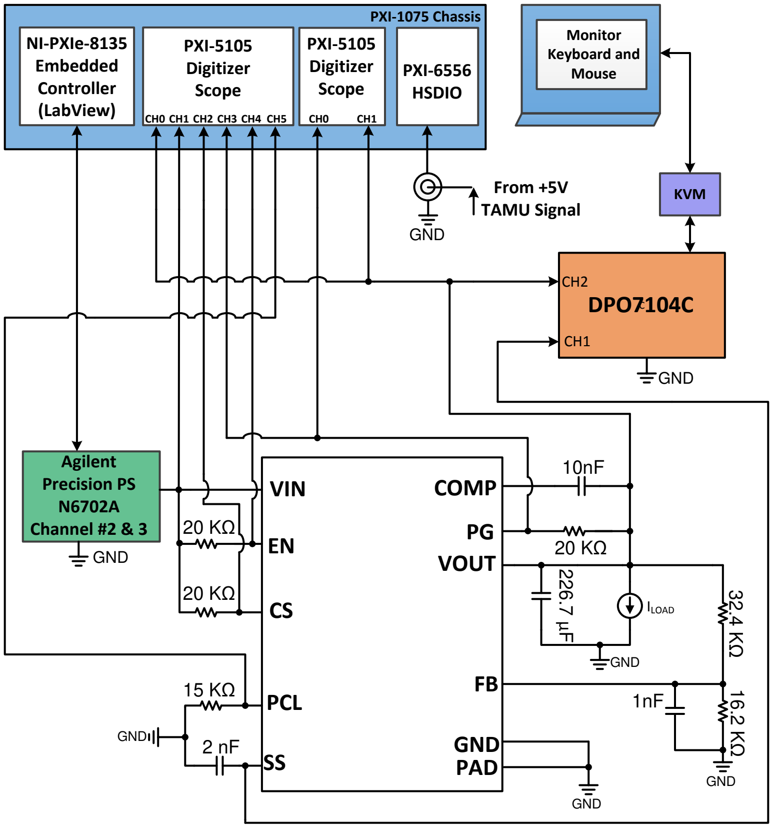

Figure 6. Block Diagram of SEE Test Setup Used for the TPS7H1101A-SP Characterization

Figure 7. Correlation Between Die and Thermocouple Temperature

7 Destructive Single Event Effects (DSEE)

7.1 Single-Event-Latchup (SEL)

SEL characterizations was performed with die temperature of 125°C. The device was heated by connecting two parallel power resistors (RP60800R0100JNBK model) attached with thermal paste to the back of the board. The temperature was monitored by attaching a K-type thermocouple to the thermal pad of the device on the top layer. Thermocouple and die correlation was verified by using a thermal IR camera prior to reaching the heavy-ions facility (TAMU). The device was exposed to a Praseodymium (Pr) heavy-ion beam incident on the die surface at 38.8° for a LET_{EFF} of 85 MeV·cm^2/mg. Flux of approximately 10^5 ions/cm^2 ·s and fluence of 5 ×10^7 ions/cm^2 were used. Run duration to achieve this fluence was approximately twelve minutes. V_{IN} was set to the maximum recommended voltage of 7 V while the output voltage was set to 5 V. Under this condition, the pass element (PMOS) was dissipating 6 Watts.

Table 5 summarizes the SEL test conditions and results. **No SEL events were observed under the test runs, indicating that the TPS7H1101-SP is SEL-immune at T = 125°C and LET_{EFF} = 85 MeV·cm^2/mg**. The SEL cross section was calculated based on zero events observed using a 95% (2σ) confidence interval (see Appendix C for discussion of the cross section calculation method). Figure 8 shows a typical current plot.

$\sigma_{SEL} \leq 7.38 \times 10^{-8}$ cm^2/device LET_{EFF} = 85 MeV·cm^2/mg, T = 125°C, 95% confidence

Table 5. Summary of TPS7H110A-SP SEL Results With T = 125°C and LET_{EFF} = 85 MeV·cm²/mg[1]

RUN NUMBER	UNIT NUMBER	TEMPERATURE (°C)	ANGLE OF INCIDENCE (°)	LET_{EFF} (MeV·cm²/mg)	FLUX (IONS/CM²·s)	FLUENCE (IONS/CM²)	V_{OUT} (V)	LOAD (A)	SEL EVENTS
1	1	125	38.8	85	8.99×10^4	5.00×10^7	5	3	0

[1] V_{IN} was set to the maximum recommended voltage of 7 V.

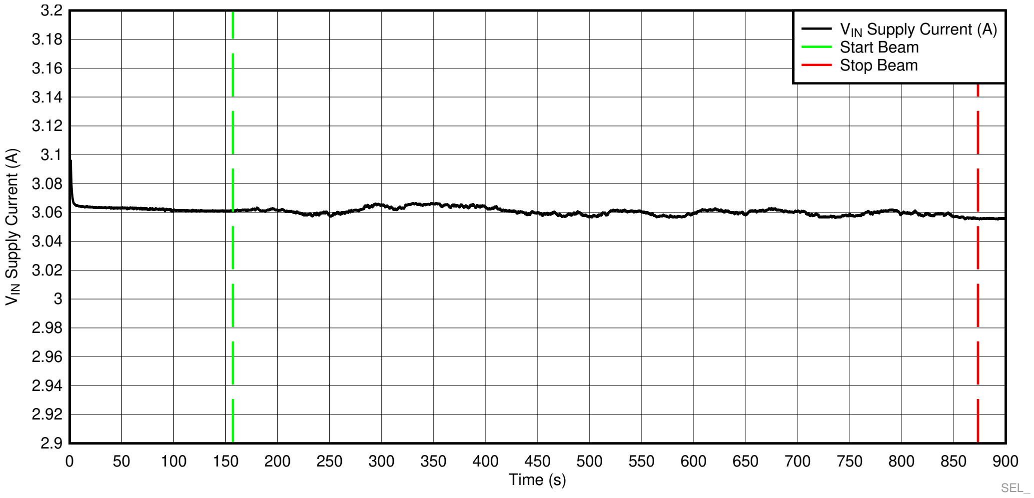

Figure 8. Current Versus Time for SEL Run #1 at T = 125ºC and 85 MeV·cm²/mg

7.2 Single-Event-Burnout (SEB) and Single-Event-Gate-Rupture (SEGR)

SEB and SEGR were performed at 20°C (No Load) to 34°C (3 Amps Load) with ^{141}Pr at an angle of incidence of 38.8º for an LET_{EFF} of 85 MeV·cm²/mg. V_{IN} was held at the maximum recommended voltage of 7 V. Flux of approximately 10^5 ions/cm²·s and fluence ≥10^7 ions/cm² was used in each run. The device was evaluated when the DUT was enabled and disabled, and loaded to 3 A at all times. Even when the device was disabled, the device had the load connected to help identify if the device was changing modes (disabled to enabled) due to heavy-ions. When the DUT was disabled, the die temperature was at room temp (approximately 20°C), however, when the part was enabled and loaded with 3 Amps, the power dissipated across the pass element (PMOS) incremented the die temperature. To test the device at low temperatures, an external cool element (vortex tube) was used during all the SEB/SEGR runs (runs 2–4). The stream of cold air was pointed at the die to chill the device during the testing, maintaining the die at 34°C at full-load, V_{IN} = 7 V, and V_{OUT} = 5 V.

Not a single change on current was observed, indicating that the TPS7H1101A-SP is SEB- and SEGR-immune at T = 20 to 34°C and LET = 85 MeV·cm²/mg. During the SEB/SEGR testing with the switch disabled (EN = GND), the current never incremented, indicating that the device never changed enable status during the exposure. Table 6 shows the conditions used for this test. Figure 9 shows a typical V_{IN} current versus time plot for runs #3. **The SEB/SEGR cross section was calculated based on zero events observed using a 95% (2σ) confidence interval and combining (or summing) fluences (see Appendix C for discussion of confidence limits).**

$\sigma_{SEB/SEGR} \leq 7.05 \times 10^{-9}$ cm²/device LET_{EFF} = 85 MeV·cm²/mg, T = 20 to 34°C, and 95% confidence

Table 6. Summary of TPS7H1101A-SP SEB and SEGR Results with T = 25°C to 34°C

RUN NUMBER	UNIT NUMBER	TEMPERATURE (°C)	ANGLE OF INCIDENCE(°)	LET_{EFF} (MeV·cm²/mg)	FLUX (IONS/CM²·s)	FLUENCE (IONS/CM²)	V_{OUT} (V)	LOAD (A)	ENABLED?	SEB/SEGR EVENTS
2	1	34	38.8	85	7.39×10^4	1×10^7	5	3	Yes	0
3	1	34	38.8	85	6.52×10^4	3×10^7	5	3	Yes	0
4	2	20	38.8	85	6.53×10^4	3×10^7	1.8	3	No	0

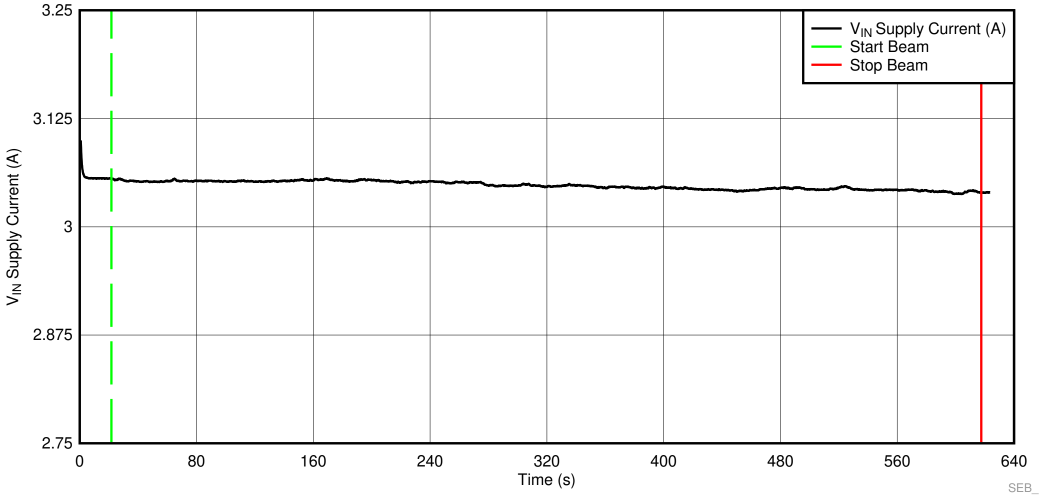

Figure 9. Current Versus Time for SEB/SEGR Run #3 at T = 34ºC and 85 MeV·cm^2/mg

8 Single Event Transients (SET)

SET testing was performed at room temperature, with ^{63}Cu ions at an angle of 50º of incidence for an LET$_{EFF}$ of 35 MeV·cm^2/mg . ^{109}Ag ions at angles of 0º and 32º of incidence were used for an LET$_{EFF}$ of 48.5 and 57 MeV·cm^2/mg, respectively. Also, ^{141}Pr ions at angles of 0º and 38.8º of incidence were used for an LET$_{EFF}$ of 61 and 85 MeV·cm^2/mg, respectively (see Table 3).

Two common different V_{IN} to V_{OUT} ratios and load currents were used for the characterization. Table 7 shows the input and output voltages and load conditions used for the SET characterization. It also shows some key observed behavior during the testing. For the SET testing, no external temperature force element was used during the characterization.

Table 7. SET Input and Output Test Conditions

V_{IN} (V)	V_{OUT} (V)	(V_{IN} - V_{OUT}) (V)	LOAD (A)	OBSERVED UPSET POLARITY	UPSETS > |10%|
5	2.5	2.5	0.5	Positive	No
5	2.5	2.5	3	Negative	No
1.8	1.2	0.6	0.5	Positive and Negative	Yes
1.8	1.2	0.6	3	Positive and Negative	Yes

Flux of approximately 10^4 ions/cm^2·s and fluence ≥ 1× 10^6 ions/cm^2 were used in each run. SETs were captured by monitoring and trigger from V_{OUT} , Power GOOD (PG), and Soft-Start (SS) pins, using three different scopes. For a detailed representation of the test setup, see Figure 6. The scope triggering from V_{OUT} was also monitoring the following:

- V_{IN}
- CS
- PG
- EN
- PCL

Scope card triggering from PG was also monitoring V_{OUT} while the scope triggering from SS was also monitoring V_{OUT}. By monitoring extras signals on the scope cards, the different SET signatures were isolated and individual cross sections were created for each one. The trigger type and value used for each signal is described in Table 8.

Table 8. Trigger Type and Value per Signal

SIGNAL NAME	SIGNAL TYPE	TRIGGER TYPE	TRIGGER VALUE (V)	TRIGGER (%)
V_{OUT} = 1.2 V	Analog	Window	2.533/2.386	±3%
V_{OUT} = 2.5 V	Analog	Window	1.229/1.211	±5%
PG	Digital	Edge/Negative	0.75, 1, and 2	-
SS	Analog	Edge/Negative	1 and 2	-

8.1 Output Voltage (V_{OUT}) SETs

8.1.1 V_{IN}= 5 V and V_{OUT} = 2.5 V

At V_{IN} = 5 V and V_{OUT} = 2.5 V, two different behaviors were observed. When the load was set to 3 Amps, all observed upsets showed a negative polarity upset. On the other hand, when the load was set to 0.5 Amps, all observed upsets were positive on polarity.

The SET cross sections were calculated based on the observed N events and a 95% (2σ) confidence interval and combining (or summing) fluences when applicable (by LET) (see Appendix C for discussion of confidence limits). The upper-bound cross section for the 0.5 and 3 Amps load is presented in Table 9 and Table 10.

Table 11 and Table 12 summarize the results for the SET characterization at V_{IN} = 5 V, V_{OUT} = 2.5 and 0.5, and 3 Amps load. Since the trigger was set to ±3% (window) of the nominal output voltage, the data was post process and categorized as ≥ |3%|, |4%|, and |5%|. For each case, a cross section plot and weibull fit was created, when applicable. Figure 10 and Figure 11 show the cross section and weibull fit for the 3 and 0.5 Amps load, respectively. The weibull fit parameters per Equation 1 are shown in Table 13.

$$X_{SECTION}(LET) = X_{SECTION-\ SATURATION} \cdot (1 - e^{\left(-\frac{LET-\ Onset}{W}\right)^{s}}) \tag{1}$$

Histograms with the normalized maximum and minimum output voltage deviation from nominal and the transient time are shown in Figure 12 to Figure 15. For each positive polarity upset, the maximum was recorded. On the other hand, for each negative polarity upset, the minimum was recorded and normalized with respect to the nominal voltage as:

$$V_{OUT}\ \ Normalized = \left(\frac{(Max\ \ or\ \ Min)\ \ Voltage - Nominal\ \ Voltage}{Nominal\ \ Voltage}\right) \cdot 100\% \tag{2}$$

Time domain plots for the worst case deviation from nominal and transient time for the 3 and 0.5 Amps load are shown in Figure 16 to Figure 18.

Table 9. Upper Bound Cross Section for V_{IN} = 5 V, V_{OUT} = 2.5 V, and Load of 3 Amps at 95% (2σ) Confidence Interval

LET_{EFF} (MeV·cm²/mg)	UPPER BOUND AT 95% (cm²)		
	SET > |3%|	SET > |4%|	SET > |5%|
48.46	1.26×10^{-6} (Based on 0 Upsets)	1.26×10^{-6} (Based on 0 Upsets)	1.26×10^{-6} (Based on 0 Upsets)
57.62	6.62×10^{-6}		
65.65	2.4×10^{-5}	2.45×10^{-6}	
84.98	2.36×10^{-5}	2.09×10^{-5}	

Table 10. Upper Bound Cross Section for V_{IN} = 5 V, V_{OUT} = 2.5 V, and Load of 0.5 Amps at 95% (2σ) Confidence Interval

LET_{EFF} (MeV·cm²/mg)	UPPER BOUND AT 95% (cm²)		
	SET > |3%|	SET > |4%|	SET > |5%|
48.46	9.44×10^{-7} (Based on 0 Upsets)	9.44×10^{-7} (Based on 0 Upsets)	9.44×10^{-7} (Based on 0 Upsets)
57.62	8.32×10^{-6}	3.46×10^{-6}	1.26×10^{-6} (Based on 0 Upsets)
65.65	2.7×10^{-5}	1.08×10^{-5}	
84.98	4.83×10^{-5}	2.24×10^{-5}	1.89×10^{-6}

Table 11. Summary of TPS7H1101A-SP SET Results at V_{IN} = 5 V, V_{OUT} = 2.5 V, and Load of 3 Amps

RUN NUMBER	UNIT NUMBER	LET_{EFF} (MeV·cm²/mg)	FLUX (ions/cm²·s)	FLUENCE (ions/cm²)	EVENTS OF SETS > |3%|	EVENTS OF SETS > |4%|	EVENTS OF SETS > |5%|
5	5	48.46	1.12×10^{4}	3×10^{6}	0	0	0
6	5	57.62	1.14×10^{4}	3×10^{6}	11	0	0
7	4	65.65	1.26×10^{4}	2.99×10^{6}	55	2	0
8	4	84.98	1.24×10^{4}	3×10^{6}	54	47	0

Table 12. Summary of TPS7H1101A-SP SET Results at V_{IN} = 5 V, V_{OUT} = 2.5 V, and Load of 0.5 Amps

RUN NUMBER	UNIT NUMBER	LET_{EFF} (MeV·cm²/mg)	FLUX (ions/cm²·s)	FLUENCE (ions/cm²)	EVENTS OF SETS > |3%|	EVENTS OF SETS > |4%|	EVENTS OF SETS > |5%|
9	5	48.46	1.19×10^{4}	3×10^{6}	0	0	0
10	5	48.46	1.19×10^{4}	1×10^{6}	0	0	0
11	5	57.62	1.18×10^{4}	3×10^{6}	15	4	0
12	4	65.65	1.28×10^{4}	2.99×10^{6}	63	21	0
13	4	84.98	1.27×10^{4}	3×10^{6}	121	51	1

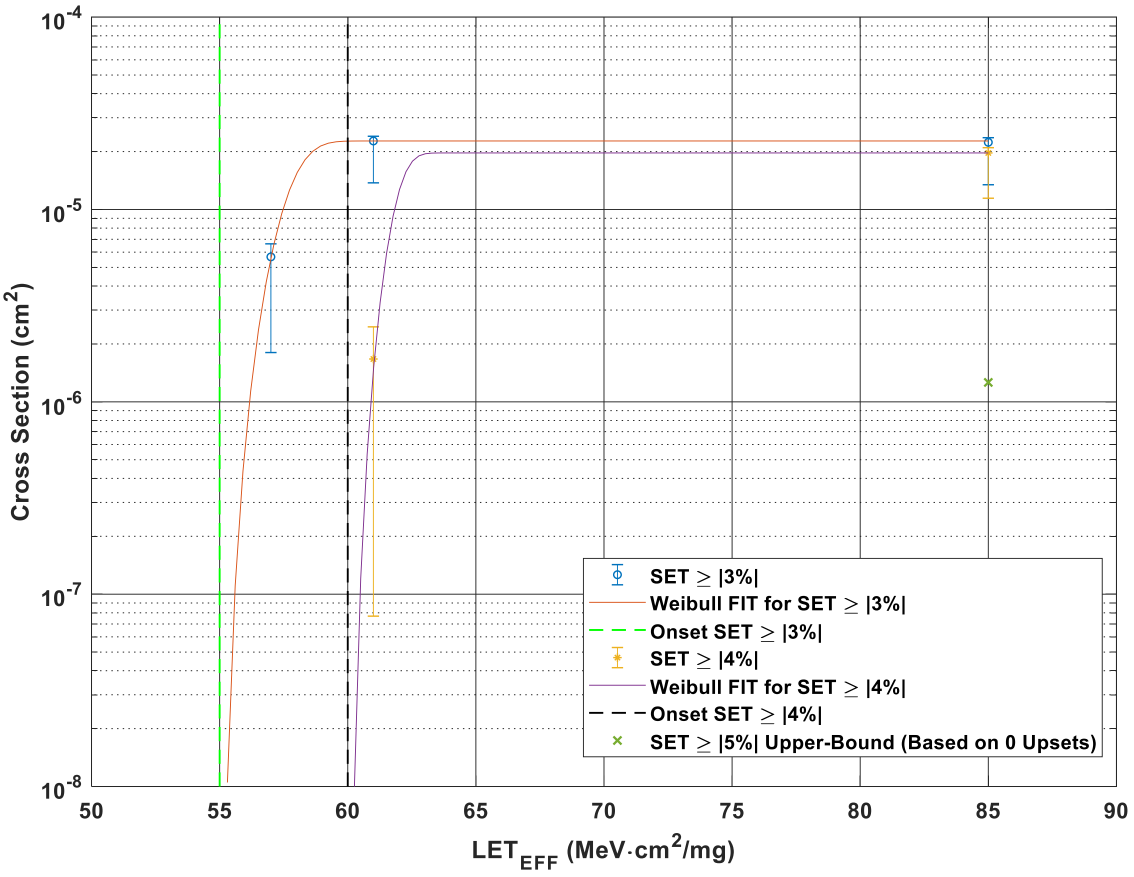

Figure 10. Cross Section Versus LET (V_{IN} = 5 V, V_{OUT} = 2.5 V, and Load = 3 A). SET ≥ |3%| on Blue, Weibull FIT for SET ≥ |3%| on Orange, Onset for SET ≥ |3%| on Green, SET ≥ |4%| on Yellow, Weibull FIT for SET ≥ |4%| on Violet, Onset for SET ≥ |4%| on Black, Upper Bound for SET ≥ |5%| on Green x (Based on 0 Observed Upsets)

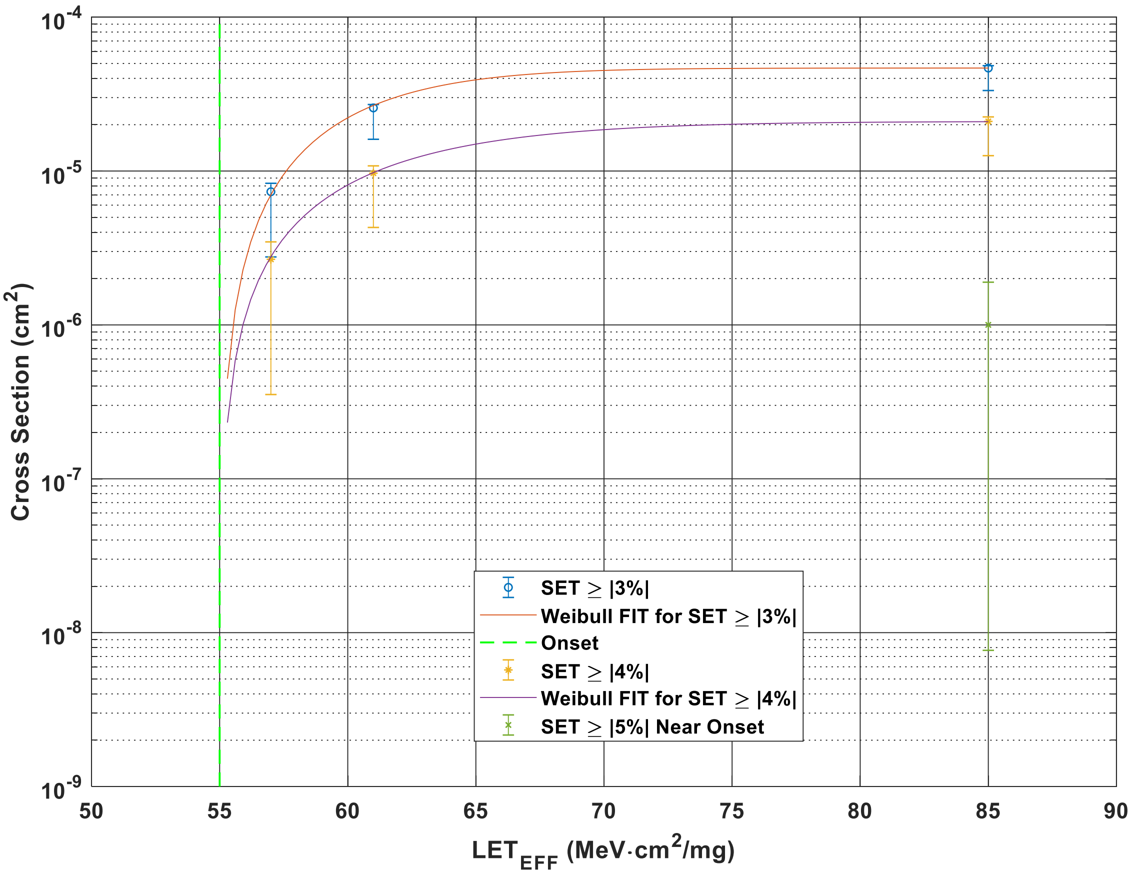

Figure 11. Cross Section Versus LET (V_{IN} = 5 V, V_{OUT} = 2.5 V, and Load= 0.5 A), SET ≥ |3%| on Blue, Weibull FIT for SET ≥ |3%| on Orange, Onset for SET ≥ |3% and 4%| on Green, SET ≥ |4%| on Yellow, Weibull FIT for SET ≥ |4%| on Violet, Near-Onset for SET ≥ |5 %| on Green

Table 13. V_{IN} = 5 V to V_{OUT} = 2.5 V Weibull Fit Parameters

PARAMETER	VALUE	LOAD (A)	CONDITION
Onset	55	3	≥ |3%|
W	2.9		
s	3.4		
σ_{SAT}	2.27×10^{-5}		
Onset	60	3	≥ |4%|
W	2		
s	3.7		
σ_{SAT}	1.97×10^{-5}		
Onset	55	0.5	≥ |3%|
W	6.7		
s	1.5		
σ_{SAT}	4.67×10^{-5}		
Onset	55	0.5	≥ |4%|
W	8.5		
s	1.35		
σ_{SAT}	2.10×10^{-5}		

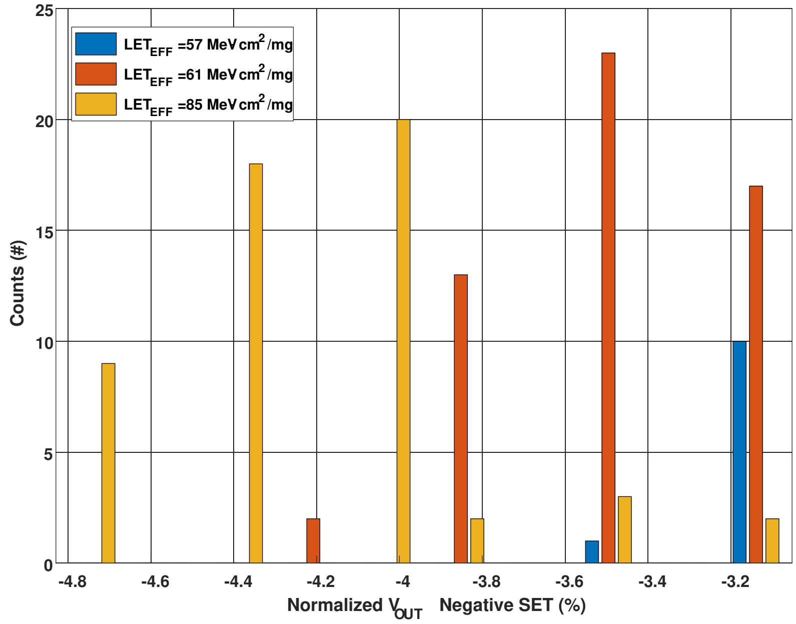

Figure 12. Normalized Output Voltage Upset Histogram of V_{IN} = 5 V, V_{OUT} = 2.5 V at Load = 3 A by LET

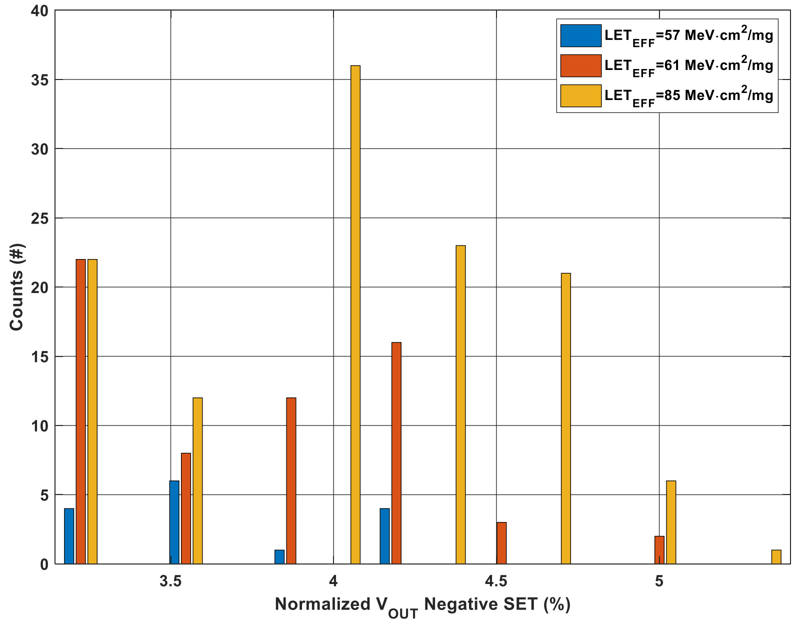

Figure 13. Normalized Output Voltage Upset Histogram of V_{IN} = 5 V, V_{OUT} = 2.5 V at Load = 0.5 A by LET

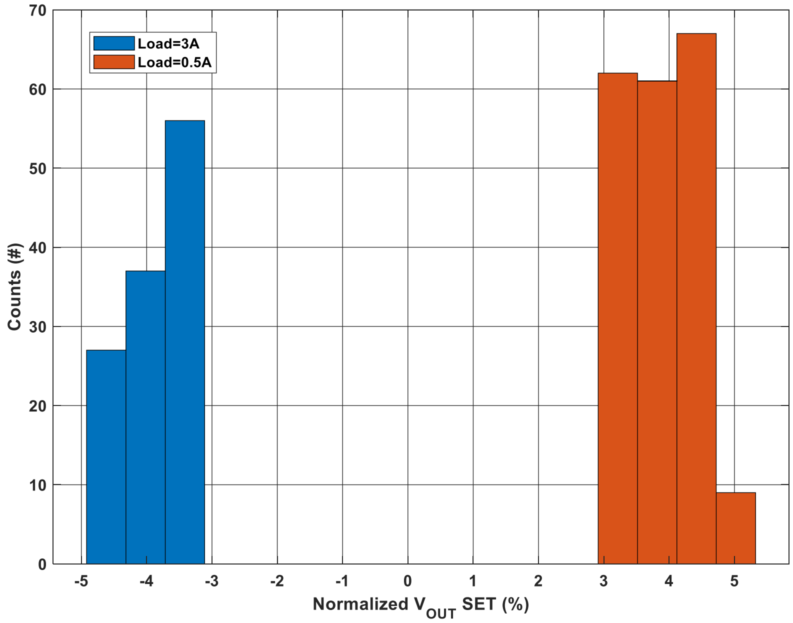

Figure 14. Normalized Output Voltage Upset Histogram of V_{IN} = 5 V, V_{OUT} = 2.5 V at Load = 0.5 and 3 A by LET

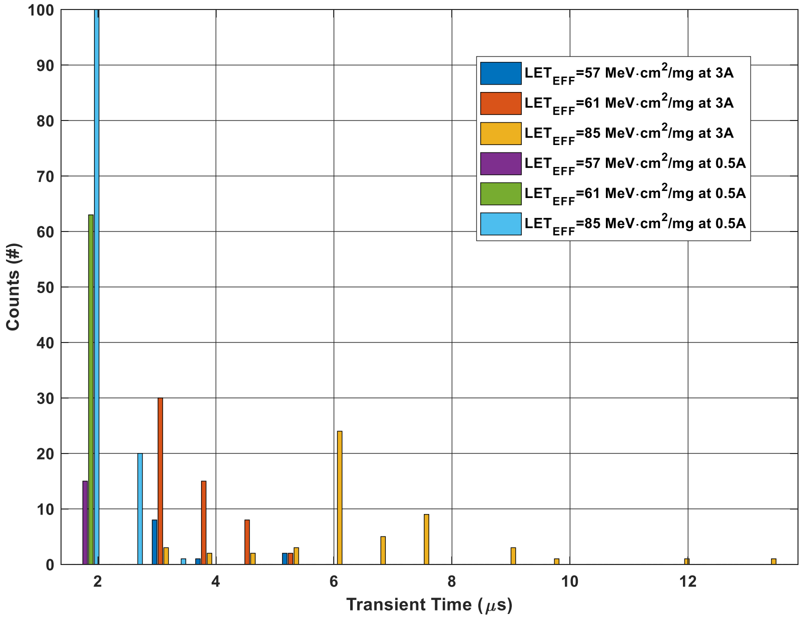

Figure 15. Transient Time Histogram of V_{IN} = 5 V, V_{OUT} = 2.5 V at Load = 0.5 and 3 A by LET

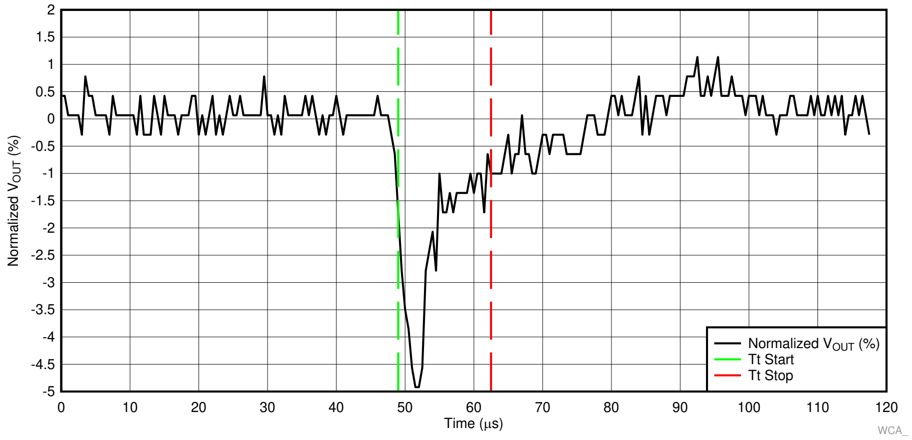

Figure 16. Worst Case Magnitude Upset and Transient Time for V_{IN} = 5 V, V_{OUT} = 2.5 V, and Load = 3 A

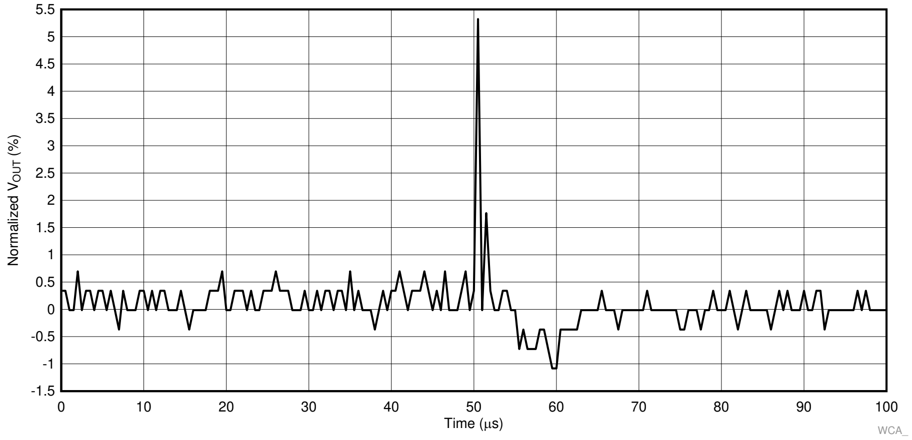

Figure 17. Worst Case Magnitude Upset for V_{IN} = 5 V, V_{OUT} = 2.5 V, and Load = 0.5 A

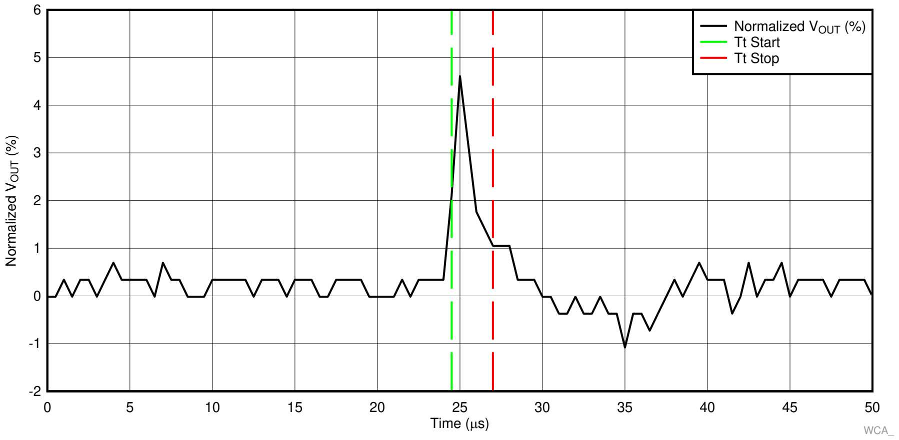

Figure 18. Worst Case Transient Time Upset for V_{IN} = 5 V, V_{OUT} = 2.5 V, and Load = 0.5 A

8.1.2 V_{IN} = 1.8 V and V_{OUT} = 1.2 V

At V_{IN} = 1.8 V and V_{OUT} = 1.2 V, positive and negative polarity upsets were observed at loads of 0.5 and 3 Amps. Some upsets exceed more than 10% from the nominal voltage (**all of these upsets were negative on polarity**). When this happens, the PG pin is pulled low. These upsets were characterized by having a longer transient time recovery when compared to those that do not exceed the 10% (typical PG threshold comparison value by design).

The SET cross section was calculated based on the observed N events and a 95% (2σ) confidence interval and combining (or summing) fluences when applicable (by LET) (see Appendix C for discussion of confidence limits). Table 14 and Table 15 presents the upper-bound cross section for the 0.5 and 3 Amps load.

Table 16 and Table 17 summarize the results for the SET characterization at V_{IN} = 1.8 V, V_{OUT} = 1.2 V, and 0.5 and 3 Amps Load. Figure 19 shows the cross section plot and Weibull fit for each load scenario. Figure 20 and Figure 21 show the cross section plot and Weibull fit for normalized output voltage transients > |10%|. These upsets have a long transient recovery time when compared with those that do not exceed the PG comparator threshold of 10%. Table 18 show the Weibull fit parameters per Equation 1.

Upsets were also categorized by upset polarity and load. Figure 22 shows the cross section plot, weibull fit, and onset for the positive and negative polarity upsets at Load = 3 A. Figure 23 shows the cross section plot, weibull fit, and onset for the positive and negative polarity upsets at Load = 0.5 A. Table 19 shows the weibull fit parameter per Equation 1.

Figure 24 to Figure 26 show histograms with the normalized maximum and minimum output voltage deviation from nominal and transient time. Voltages were normalized as shown in Equation 2. Figure 27 to Figure 31 present worst case time domain plots.

Table 14. Upper Bound Cross Section for V_{IN} = 1.8 V, V_{OUT} = 1.2 V, and Load of 3 Amps at 95% (2σ) Confidence Interval

LET_{EFF} (MeV·cm^2/mg)	UPPER BOUND AT 95% (cm^2)	
	SET > |5%|	SET > |10%| (P_{GOOD} FLAG)
32.63	1.26×10^{-6} (Based on 0 Upsets)	Not Available
48.46	1.47×10^{-5}	1.97×10^{-6}
57.62	7.67×10^{-5}	3.46×10^{-6}
65.65	6.05×10^{-5}	3.95×10^{-6}
84.98	8.14×10^{-5}	6.63×10^{-6}

Table 15. Upper Bound Cross Section for V_{IN} = 1.8 V, V_{OUT} = 1.2 V, and Load of 0.5 Amps at 95% (2σ) Confidence Interval

LET_{EFF} (MeV·cm^2/mg)	UPPER BOUND AT 95% (cm^2)	
	SET > |5%|	SET > |10%| (P_{GOOD} FLAG)
32.63	3.78×10^{-6} (Based on 0 Upsets)	Not Available
48.46	1.26×10^{-6} (Based on 0 Upsets)	2.97×10^{-6}
57.62	1.89×10^{-6}	1.89×10^{-6}
65.65	6.18×10^{-6}	
84.98	1.11×10^{-5}	3.99×10^{-6}

Table 16. Summary of TPS7H1101A-SP SET Results at V_{IN} = 1.8 V, V_{OUT} = 1.2 V, and Load of 3 Amps(1)

RUN NUMBER	UNIT NUMBER	LET_{EFF} (MeV·cm²/mg)	FLUX (ions/cm²·s)	FLUENCE (ions/cm²)	TRIGGER SIGNAL	SETS EVENTS > |5%|	SETS EVENTS > |10%| (P_{GOOD} FLAG)
14	5	32.63	9.71×10^3	1×10^6	V_{OUT}	0	0
15	5	32.63	9.65×10^3	2×10^6	V_{OUT}	0	0
16	5	48.46	9.94×10^3	3×10^6	V_{OUT}	31	3
17	5	48.46	9.96×10^3	3×10^6	PG	N/A	2
18	5	57.62	1.16×10^4	3×10^6	V_{OUT}	200	0
19	5	57.62	1.01×10^4	3×10^6	PG	N/A	4
20	3	65.65	9.29×10^3	3×10^6	V_{OUT}	166	4
21	3	65.65	9.63×10^3	3×10^6	V_{OUT}	159	10
22	3	84.98	1.09×10^4	3×10^6	V_{OUT}	209	3
23	3	84.98	9.13×10^3	3×10^6	V_{OUT}	471	8

(1) The data presented here was collected at room temperature and load of 3 Amps.

Table 17. Summary of TPS7H1101A-SP SET Results at V_{IN} = 1.8 V, V_{OUT} = 1.2 V, and Load of 0.5 Amps(1)

RUN NUMBER	UNIT NUMBER	LET_{EFF} (MeV·cm²/mg)	FLUX (ions/cm²·s)	FLUENCE (ions/cm²)	TRIGGER SIGNAL	SETSEVENTS > |5%|	SETS EVENTS > |10%| (P_{GOOD} FLAG)
24	5	32.63	9.4×10^3	1×10^6	V_{OUT}	0	0
25	5	48.46	9.7×10^3	3×10^6	V_{OUT}	0	0
26	5	48.46	9.97×10^3	3×10^6	PG	N/A	3
27	5	57.62	1.13×10^4	3×10^6	V_{OUT}	1	1
28	5	57.62	1.13×10^4	3×10^6	PG	N/A	0
29	3	65.65	8.95×10^3	3×10^6	V_{OUT}	1	1
30	3	84.98	9.8×10^3	3×10^6	V_{OUT}	8	6
31	3	84.98	9.22×10^3	9.99×10^5	V_{OUT}	3	2

(1) The data presented here was collected at room temperature and load of 0.5 Amps.

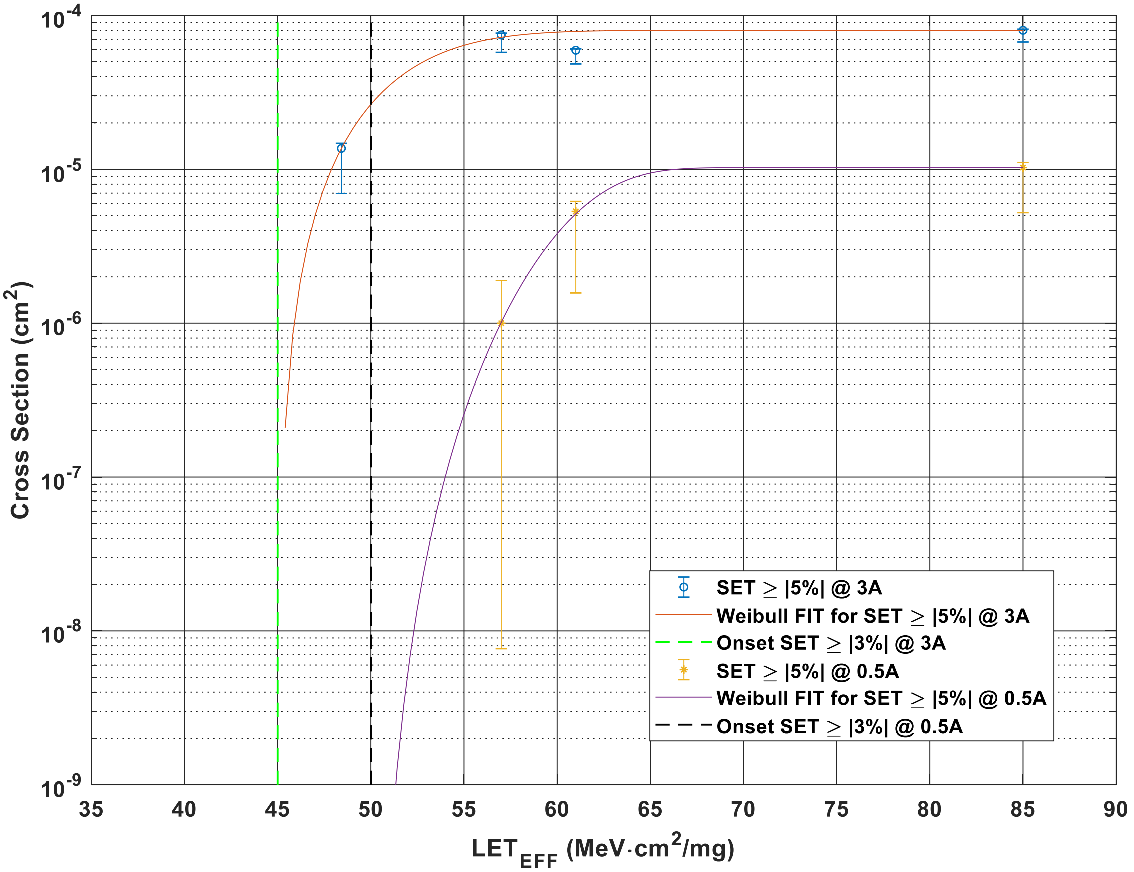

Figure 19. Cross Section versus LET (V_{IN} = 1.8 V, V_{OUT} = 1.2 V, and Load = 3 and 0.5 A), SET ≥ |5%| at 3 A on Blue, Weibull FIT for SET ≥ |5%| at 3 A on Orange, Onset for SET ≥ |5%| at 3 A on Green, SET ≥ |5%| at 0.5 A on Yellow, Weibull FIT for SET ≥ |5%| at 0.5 A on Violet, Onset for SET ≥ |5%| at 0.5 A on Black

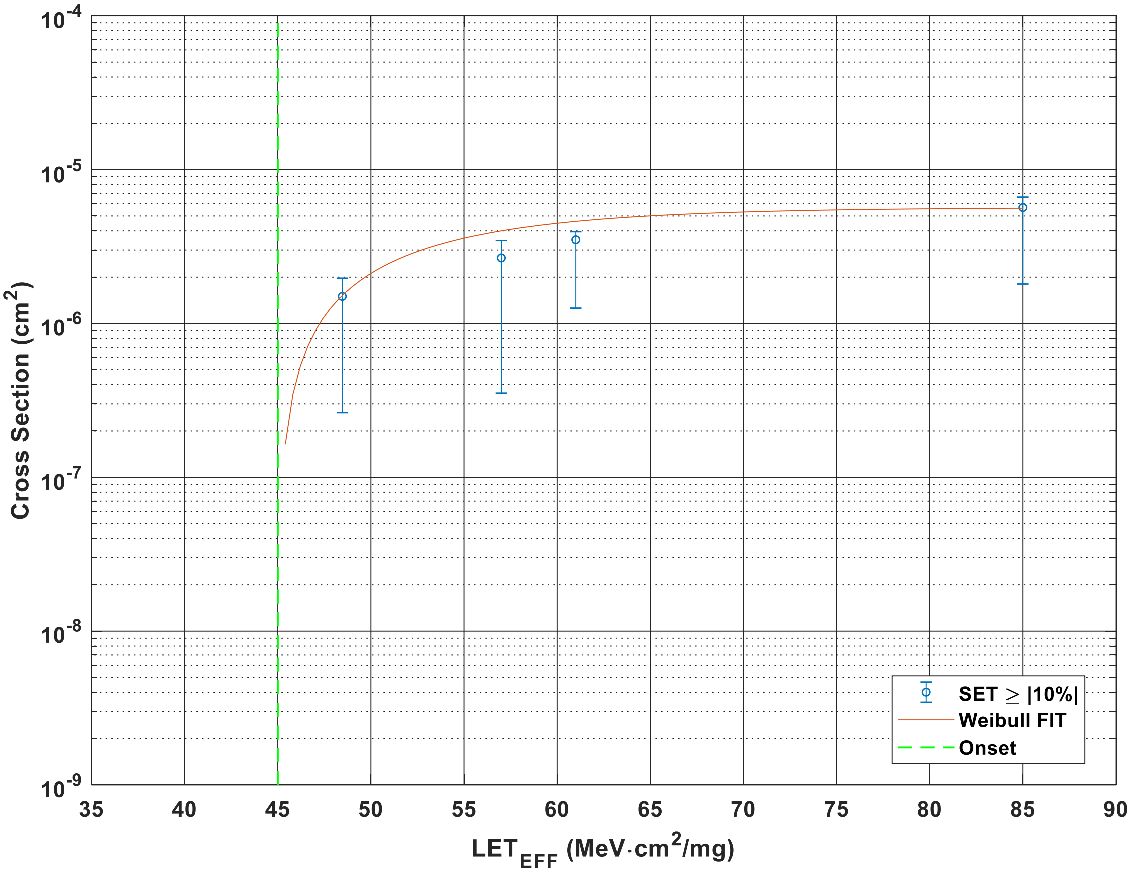

Figure 20. Cross Section versus LET (V_{IN} = 1.8 V, V_{OUT} = 1.2 V, and Load = 3 A) for SET < -10%, SET ≥ |10%| at 3 A on Blue, Weibull FIT for SET ≥ |10%| at 3 A on Orange, Onset for SET ≥ |10%| at 3 A on Green

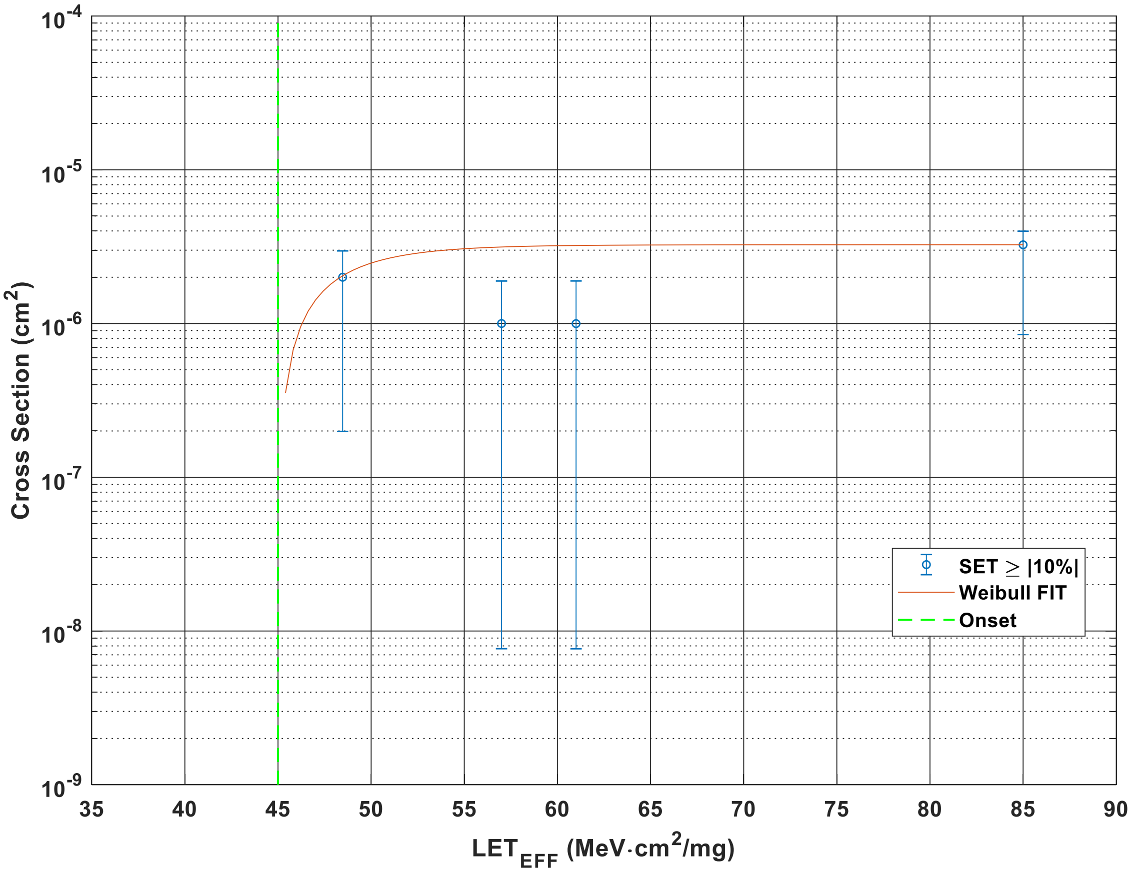

Figure 21. Cross Section versus LET (V_{IN} = 1.8 V, V_{OUT} = 1.2 V, and Load = 0.5 A) for SET < -10%, SET ≥ |10%| on Blue, Weibull FIT for SET ≥ |10%| on Orange, Onset for SET ≥ |10%| on Green

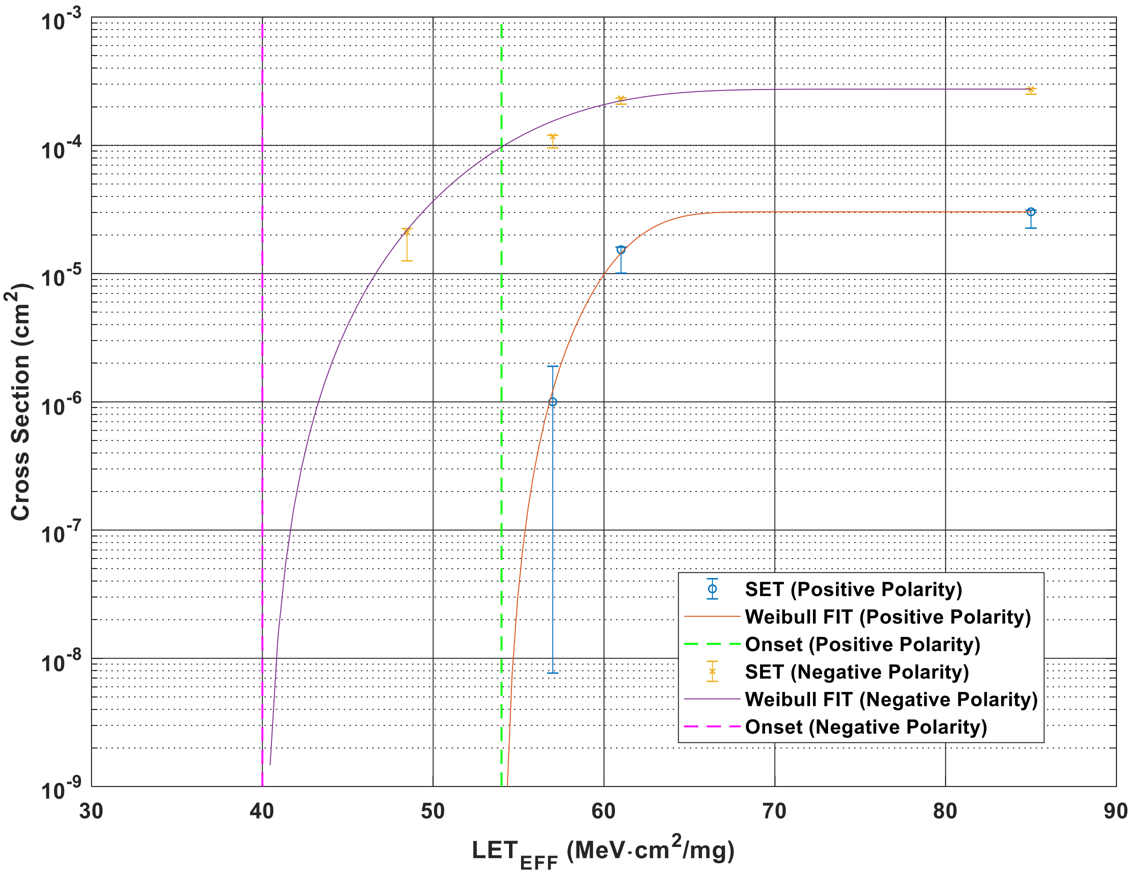

Figure 22. Cross Section versus LET (V_{IN} = 1.8 V, V_{OUT} = 1.2 V, and Load = 3 A) for Positive and Negative Polarity Upsets, SET $X_{SECTION}$ with Positive Polarity on Blue, Weibull FIT for Positive Polarity on Orange, Onset for Positive Polarity on Green, SET $X_{SECTION}$ with Negative Polarity on Yellow, Weibull FIT for Negative Polarity on Violet, Onset for Negative Polarity on Magenta

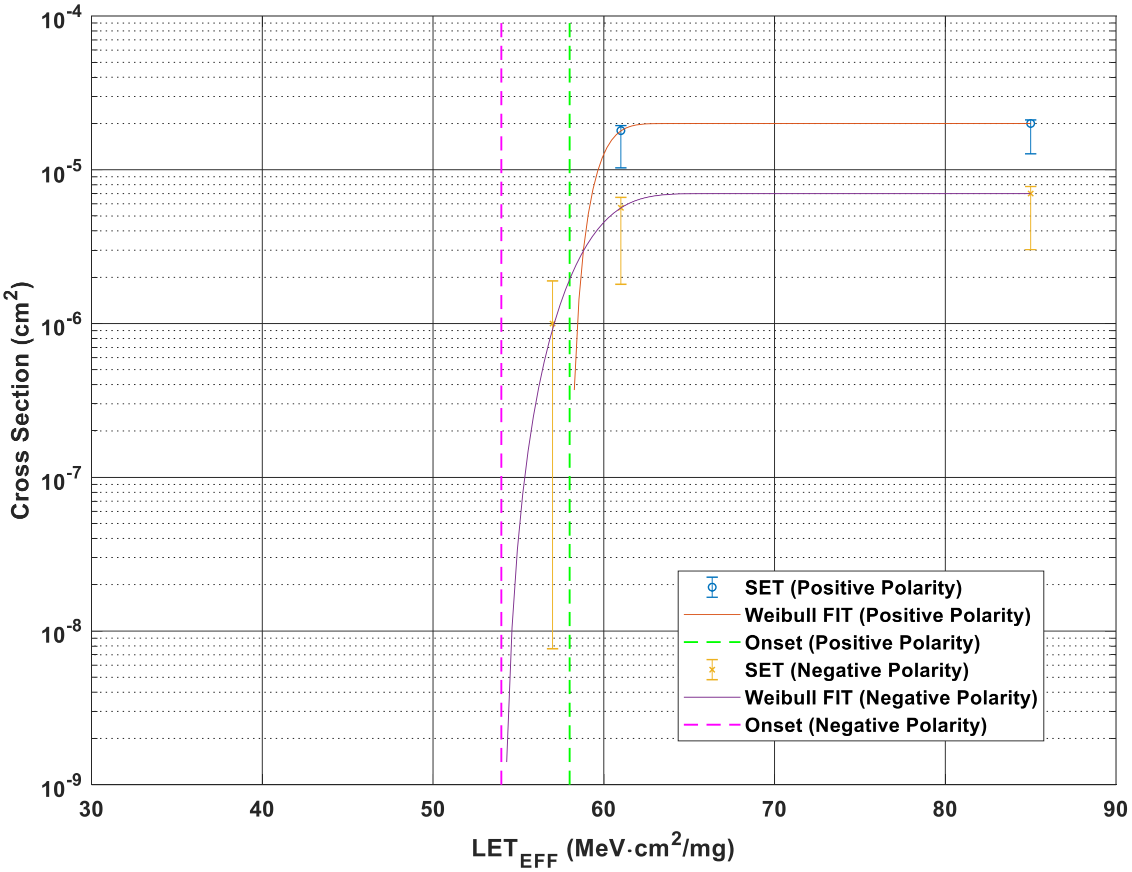

Figure 23. Cross Section versus LET (V_{IN} = 1.8 V, V_{OUT} = 1.2 V, and Load =0.5 A) for Positive and Negative Polarity Upsets, SET $X_{SECTION}$ with Positive Polarity on Blue, Weibull FIT for Positive Polarity on Orange, Onset for Positive Polarity on Green, SET $X_{SECTION}$ with Negative Polarity on Yellow, Weibull FIT for Negative Polarity on Violet, Onset for Negative Polarity on Magenta.

Table 18. V_{IN} = 1.8 V to V_{OUT} = 1.2 V Weibull Fit Parameters (Categorized by Load and Percentage)

PARAMETER	VALUE	LOAD (A)	CONDITION
Onset	45	3	SET>|5%|
W	7.9		
s	2		
σ_{SAT}	8×10^{-5}		
Onset	50	0.5	SET>|5%|
W	12		
s	4.2		
σ_{SAT}	1.03×10^{-5}		
Onset	45	3	SET>|10%|
W	10		
s	1.1		
σ_{SAT}	5.67×10^{-6}		
Onset	45	0.5	SET>|10%|
W	3.5		
s	1		
σ_{SAT}	3.25×10^{-6}		

Table 19. V_{IN} = 1.8 V to V_{OUT} = 1.2 V Weibull Fit Parameters (Categorized by Polarity)

PARAMETER	VALUE	LOAD (A)	CONDITION
Onset	54	3	Positive Polarity
W	8		
s	3.25		
σ_{SAT}	3.03×10^{-5}		
Onset	40	3	Negative Polarity
W	1.8		
s	3.3		
σ_{SAT}	2.75×10^{-4}		
Onset	58	0.5	Positive Polarity
W	2		
s	2		
σ_{SAT}	2×10^{-5}		
Onset	54	0.5	Negative Polarity
W	5.9		
s	2.9		
σ_{SAT}	7×10^{-6}		

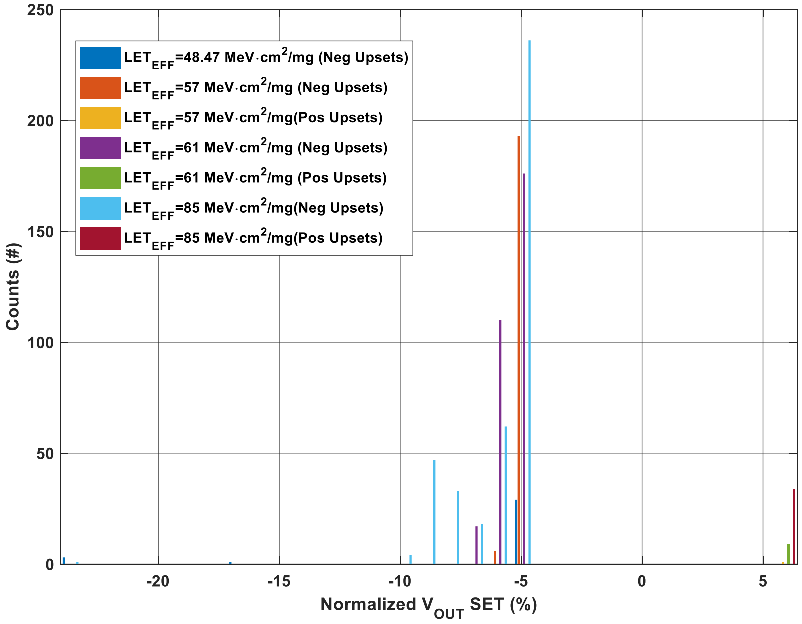

Figure 24. Normalized Output Voltage Upset Histogram of V_{IN} = 1.8 V, V_{OUT} = 1.2 V at Load = 3 A by LET

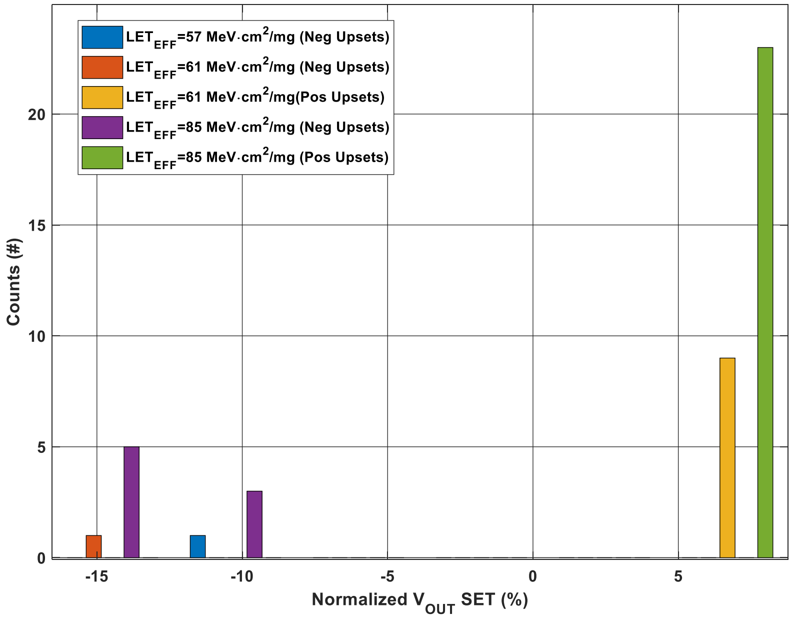

Figure 25. Normalized Output Voltage Upset Histogram of V_{IN} = 1.8 V, V_{OUT} = 1.2 V at Load = 0.5 A by LET

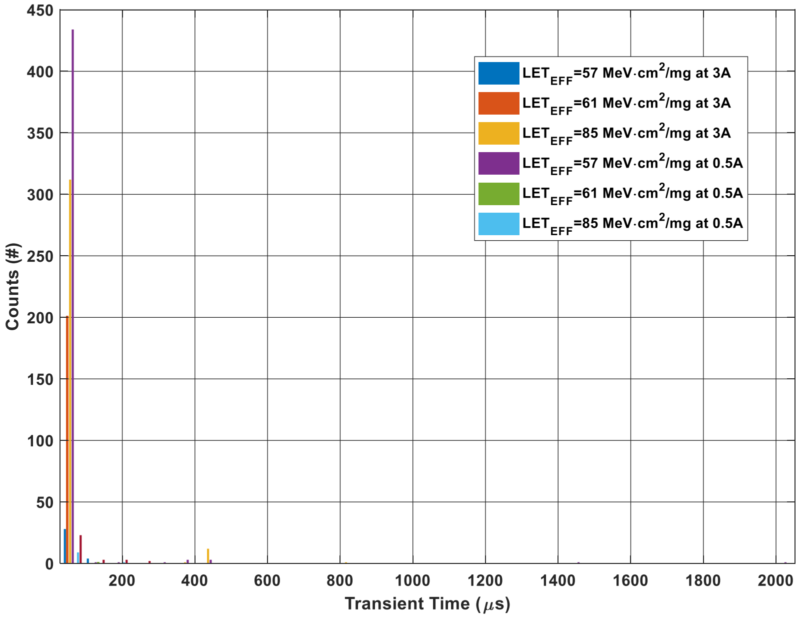

Figure 26. Transient Time Histogram of V_{IN} = 1.2 V, V_{OUT} = 1.2 V at Load = 0.5 A by LET

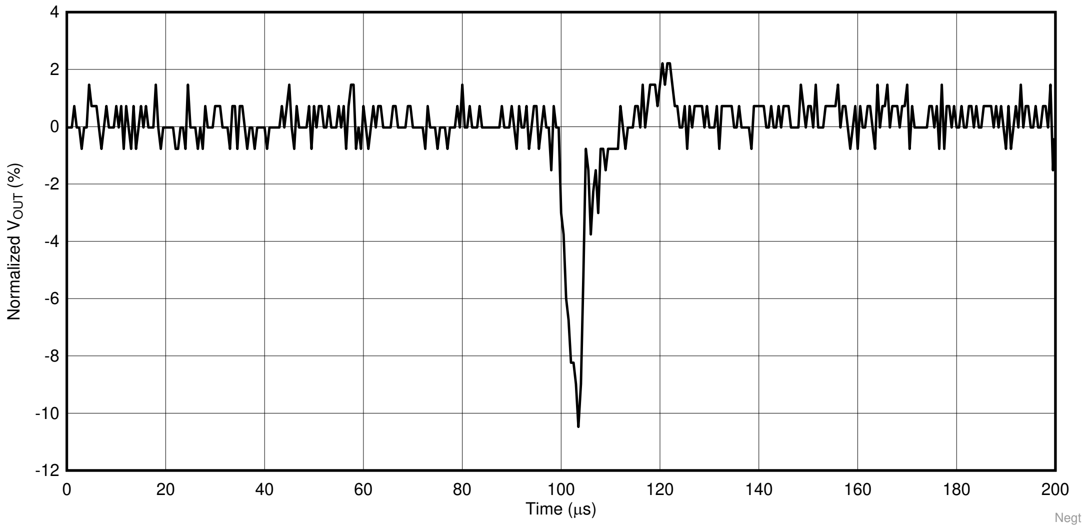

Figure 27. Worst Case Magnitude for Negative Polarity Upset at V_{IN} = 1.8 V, V_{OUT} = 1.2, and Load = 3 A

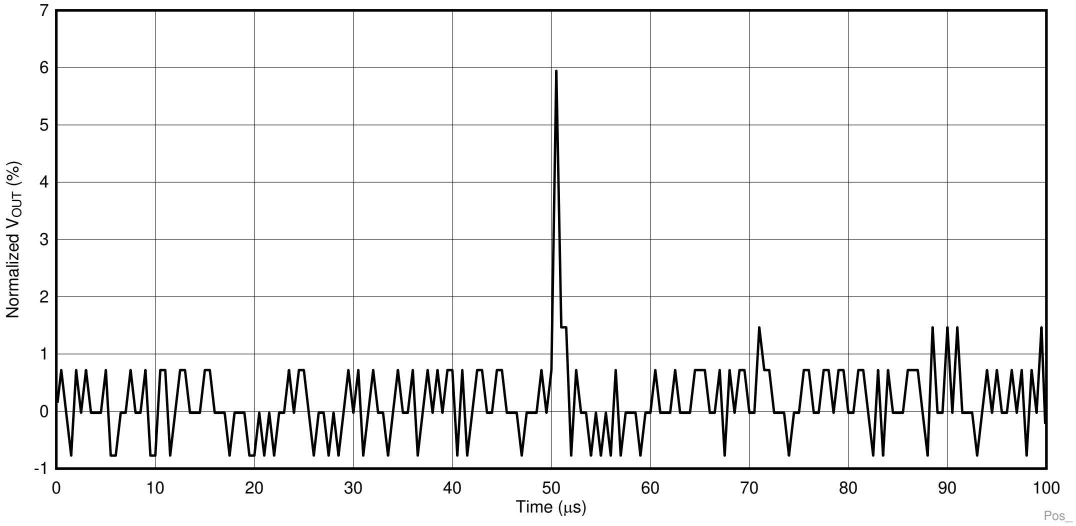

Figure 28. Worst Case Magnitude for Positive Polarity Upset at V_{IN} = 1.8 V, V_{OUT} = 1.2, and Load = 3 A

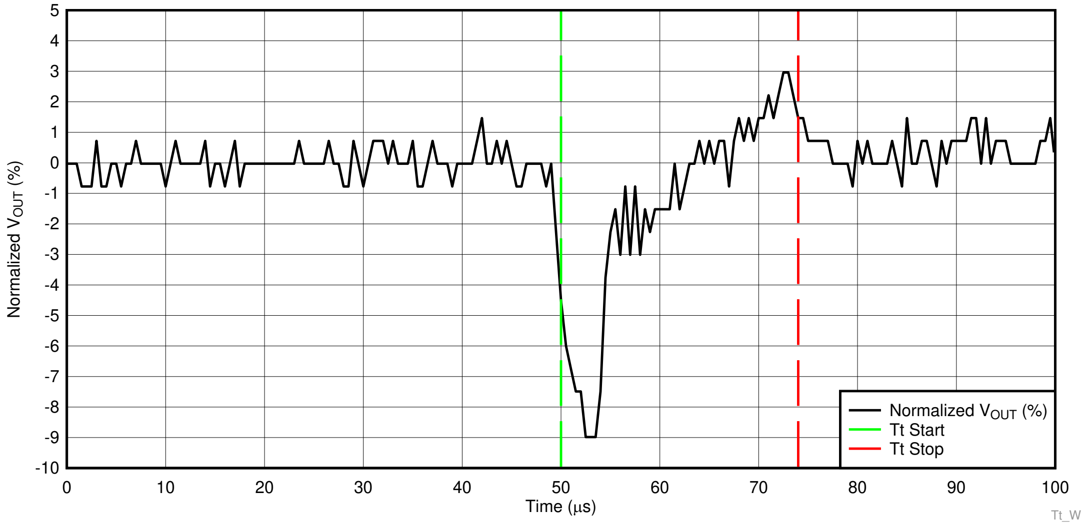

Figure 29. Worst Case Transient Time Upset for V_{IN} = 1.8 V, V_{OUT} = 1.2 V, and Load = 3 A

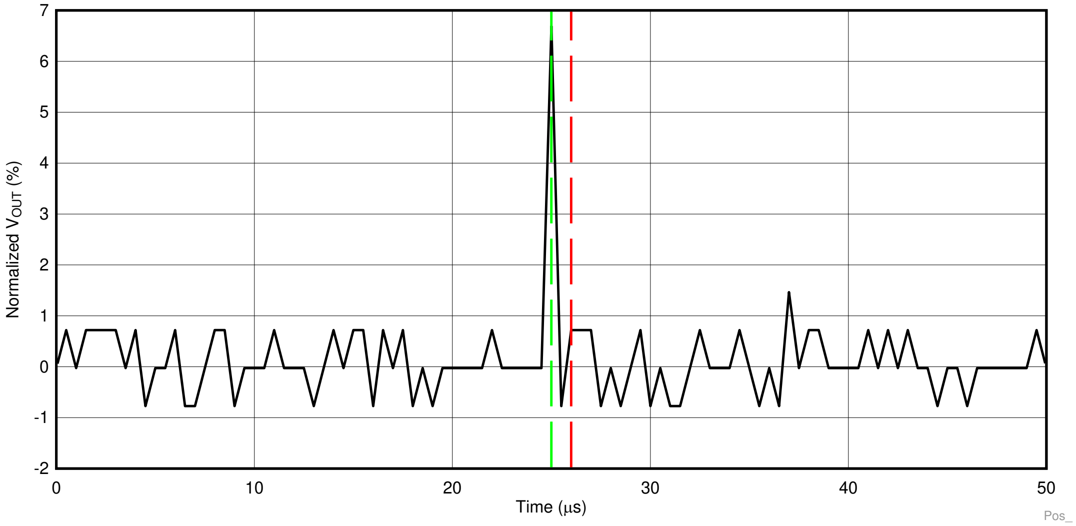

Figure 30. Worst Case Magnitude for Positive Polarity Upset and Transient Time at V_{IN} = 1.8 V, V_{OUT} = 1.2, and Load = 0.5 A

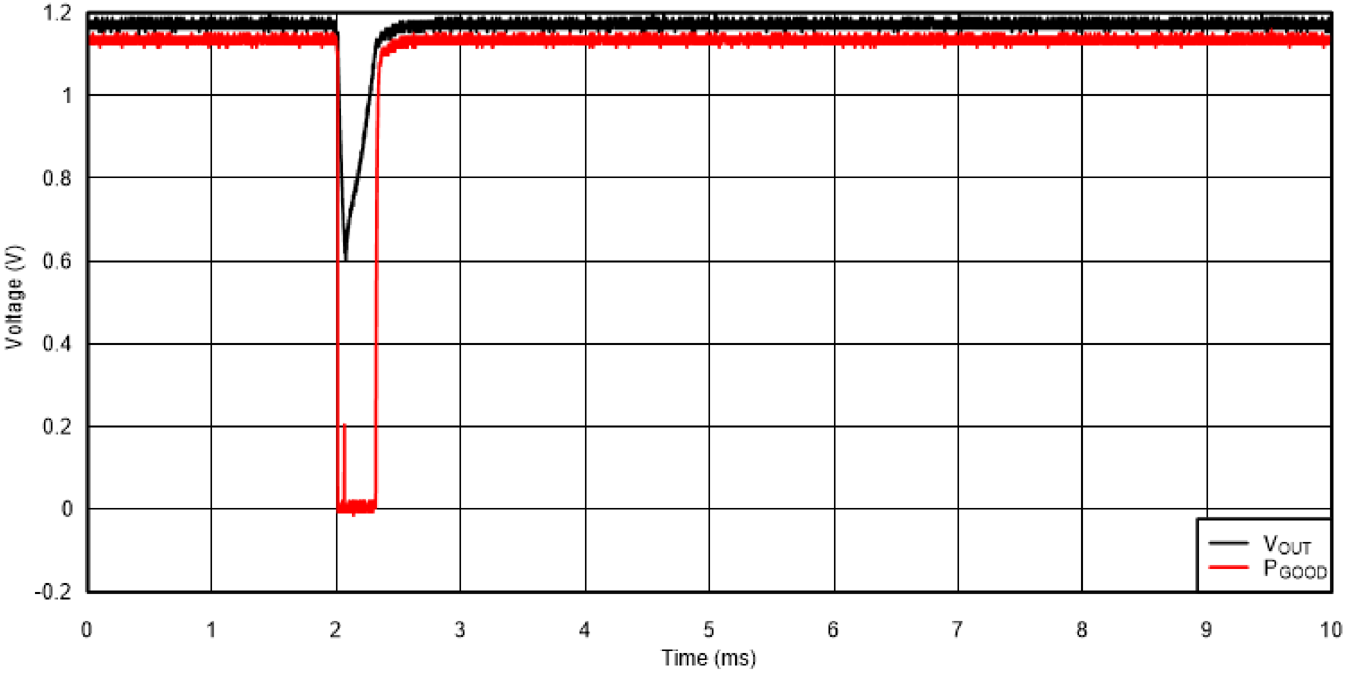

This upset represents the worst case across the 3 and 0.5 Amps load used for the characterization.

Figure 31. Worst Case Observed Negative Polarity Upset and Transient Time at V_{IN} = 1.8 V, V_{OUT} = 1.2, That Exceeded 10% from the Nominal Output Voltage

8.2 Power Good (PG) SETs

In any run presented in Section 8.1.1 and Section 8.1.2, **not a single PGOOD SET was observed**. All PGOOD flips were the manifestation by the design behavior. Combining the fluence of all runs at 85 MeV·cm^2/mg, the upper-bound cross section based on **zero observed events and using a 95% (2σ) confidence interval (see Appendix C for discussion of confidence limits) is:**

$\sigma_{PGOOD} \leq 2.36 \times 10^{-7}$ cm^2/device LET_{EFF} = 85 MeV·cm^2/mg, T = Room Temp and 95% confidence (3)

8.3 Soft-Start (SS) SETs

During run #22, a single SS SET was observed. This upset is characterized by having a long recovery or transient time, mostly dominated by the Soft-Start Capacitor. During this offset, the output voltage collapses to zero and self starts (recovers) going back to the programmed voltage. The upper bound cross section based on **one observed events and using a 95% (2σ) confidence interval (see Appendix C for discussion of confidence limits) is:**

$\sigma_{Soft\text{-}Start} \leq 1.09 \times 10^{-6}$ cm^2/device LET_{EFF} = 85 MeV·cm^2/mg, T = Room Temp and 95% confidence (4)

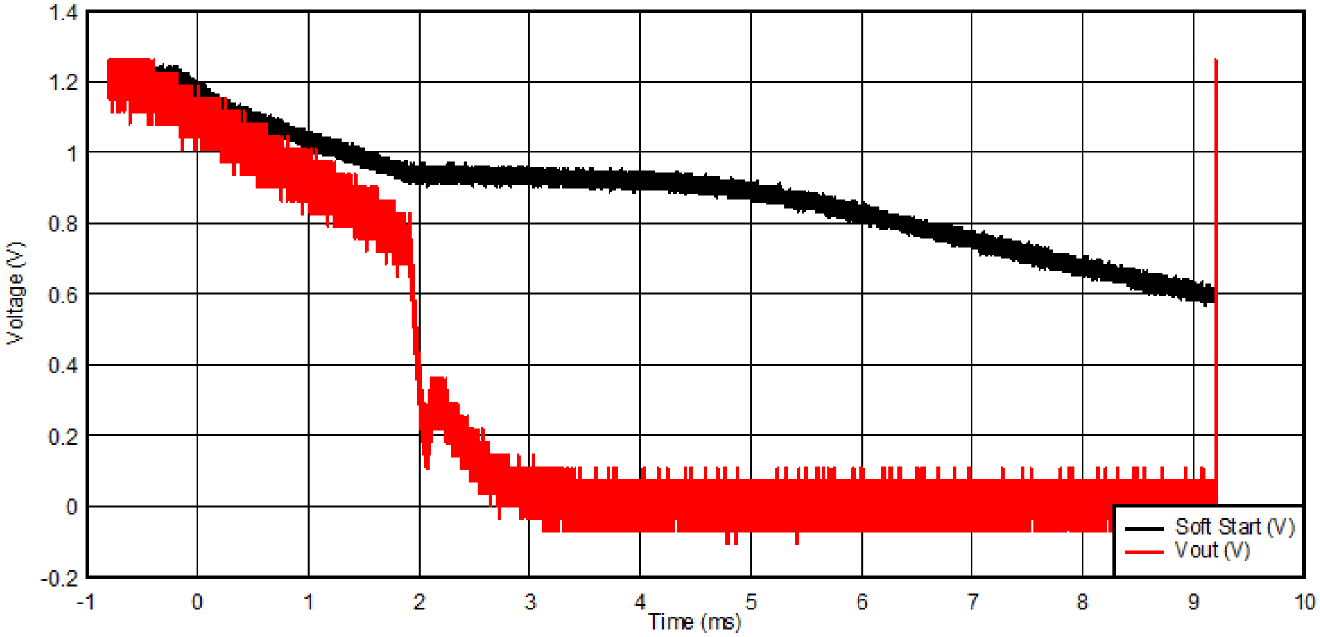

This type of SET was observed just once at 85 MeV·cm^2/mg, V_{IN} = 1.8 V, V_{OUT} = 1.2, and Load = 3 A.

Figure 32. Soft-Start Upset at V_{IN} = 1.8 V, V_{OUT} = 1.2 V, and 3 Amps Load During Run #22

9 Event Rate Calculations

Events rates were calculated for LEO (ISS) and GEO environments by combining CREME96 orbital integral flux estimations. A minimum shielding of 100 mils (2.54 mm) of aluminum and "worst week" solar activity were assumed. "Worst Week" is similar to 99% upper bound for the environment. With **zero upsets** for SEL, SEB, PGOOD, and SET at VIN = 5 V, VOUT = 2.5, and Load = 3 Amps, the error rate was calculated using the upper bound cross section and the integral flux at 85 MeV·cm^2/mg. Otherwise, the respective on-set and the upper bound at 85 MeV·cm^2/mg was used. To be conservative, all rate calculations were done using the upper-bound, even when the upset rate is greater than zero.

Table 20. SEL Event Rate Calculations for Worst-Case LEO and GEO Orbits

ORBIT TYPE	ONSET LET_{EFF} (MeV·cm^2/mg)	CREME96 INTEGRAL FLUX (/day·cm^2)	SATURATION CROSS SECTION (cm^2)	EVENT RATE (/DAY)	EVENT RATE (FIT)	MTBE (YEARS)
LEO (ISS)	85	2.43×10^{-5}	7.38×10^{-8}	1.79×10^{-12}	7.48×10^{-5}	1.52×10^{9}
GEO		6.81×10^{-5}		5.02×10^{-12}	2.09×10^{-4}	5.44×10^{8}

Table 21. SEB/SEGR Event Rate Calculations for Worst-Case LEO and GEO Orbits

ORBIT TYPE	ONSET LET_{EFF} (MeV·cm^2/mg)	CREME96 INTEGRAL FLUX (/day·cm^2)	SATURATION CROSS SECTION (cm^2)	EVENT RATE (/DAY)	EVENT RATE (FIT)	MTBE (YEARS)
LEO (ISS)	85	2.43×10^{-5}	7.05×10^{-9}	1.72×10^{-13}	7.15×10^{-6}	1.59×10^{10}
GEO		6.81×10^{-5}		4.8×10^{-13}	2×10^{-5}	5.7×10^{9}

Table 22. SET Event Rate Calculations for Worst-Case LEO and GEO Orbits at VIN = 5 V, VOUT = 2.5 V, Load = 3 A, and SET ≥ |3|% from the Nominal Output Voltage

ORBIT TYPE	ONSET LET$_{EFF}$ (MeV·cm^2/mg)	CREME96 INTEGRAL FLUX (/day·cm^2)	SATURATION CROSS-SECTION (cm^2)	EVENT RATE (/DAY)	EVENT RATE (FIT)	MTBE (YEARS)
LEO (ISS)	55	2.7 x 10^{-4}	2.36 x 10^{-5}	6.4 x 10^{-9}	0.2654	4.3 x 10^{5}
GEO		8.49 x 10^{-4}		2 x 10^{-8}	0.835	1.36 x 10^{5}

Table 23. SET Event Rate Calculations for Worst-Case LEO and GEO Orbits at VIN = 5 V, VOUT = 2.5 V, Load = 3 A, and SET ≥ |4|% from the Nominal Output Voltage

ORBIT TYPE	ONSET LET$_{EFF}$ (MeV·cm^2/mg)	CREME96 INTEGRAL FLUX (/day·cm^2)	SATURATION CROSS-SECTION (cm^2)	EVENT RATE (/DAY)	EVENT RATE (FIT)	MTBE (YEARS)
LEO (ISS)	60	1.67 x 10^{-4}	2.09 x 10^{-5}	3.48 x 10^{-9}	0.1452	7.86 x 10^{5}
GEO		4.93 x 10^{-4}		1.03 x 10^{-8}	0.4301	2.65 x 10^{5}

Table 24. SET Event Rate Calculations for Worst-Case LEO and GEO Orbits at VIN = 5 V, VOUT = 2.5 V, Load = 3 A, and SET ≥ |5|% from the Nominal Output Voltage

ORBIT TYPE	ONSET LET$_{EFF}$ (MeV·cm^2/mg)	CREME96 INTEGRAL FLUX (/day·cm^2)	SATURATION CROSS-SECTION (cm^2)	EVENT RATE (/DAY)	EVENT RATE (FIT)	MTBE (YEARS)
LEO (ISS)	85	2.43 x 10^{-5}	1.26 x 10^{-6}	3.06 x 10^{-11}	0.0013	8.93 x 10^{7}
GEO		6.81 x 10^{-5}		8.58 x 10^{-11}	0.0036	3.19 x 10^{7}

Table 25. SET Event Rate Calculations for Worst-Case LEO and GEO Orbits at VIN = 5 V, VOUT = 2.5 V, Load = 0.5 A, and SET ≥ |3|% from the Nominal Output Voltage

ORBIT TYPE	ONSET LET$_{EFF}$ (MeV·cm^2/mg)	CREME96 INTEGRAL FLUX (/day·cm^2)	SATURATION CROSS-SECTION (cm^2)	EVENT RATE (/DAY)	EVENT RATE (FIT)	MTBE (YEARS)
LEO (ISS)	55	2.69 x 10^{-4}	4.83 x 10^{-5}	1.3 x 10^{-8}	0.5432	2.1 x 10^{5}
GEO		8.49 x 10^{-4}		4.1 x 10^{-8}	1.71	6.68 x 10^{4}

Table 26. SET Event Rate Calculations for Worst-Case LEO and GEO Orbits at VIN = 5 V, VOUT = 2.5 V, Load = 0.5 A, and SET ≥ |4|% from the Nominal Output Voltage

ORBIT TYPE	ONSET LET$_{EFF}$ (MeV·cm^2/mg)	CREME96 INTEGRAL FLUX (/day·cm^2)	SATURATION CROSS-SECTION (cm^2)	EVENT RATE (/DAY)	EVENT RATE (FIT)	MTBE (YEARS)
LEO (ISS)	55	2.69 x 10^{-4}	2.24 x 10^{-5}	6.04 x 10^{-9}	0.2519	4.53 x 10^{5}
GEO		8.49 x 10^{-4}		1.90 x 10^{-8}	0.7926	1.44 x 10^{5}

Table 27. SET Event Rate Calculations for Worst-Case LEO and GEO Orbits at VIN = 5 V, VOUT = 2.5 V, Load = 0.5 A, and SET ≥ |5|% from the Nominal Output Voltage

ORBIT TYPE	ONSET LET$_{EFF}$ (MeV·cm^2/mg)	CREME96 INTEGRAL FLUX (/day·cm^2)	SATURATION CROSS-SECTION (cm^2)	EVENT RATE (/DAY)	EVENT RATE (FIT)	MTBE (YEARS)
LEO (ISS)	85	2.43 x 10^{-5}	1.89 x 10^{-6}	4.6 x 10^{-11}	0.0019	5.95 x 10^{7}
GEO		6.81 x 10^{-5}		1.29 x 10^{-10}	0.0054	2.13 x 10^{7}

Table 28. SET Event Rate Calculations for Worst-Case LEO and GEO Orbits at VIN = 1.8 V, VOUT = 1.2 V, Load = 3 A, and SET ≥ |5|% from the Nominal Output Voltage

ORBIT TYPE	ONSET LET_{EFF} ($MeV \cdot cm^2/mg$)	CREME96 INTEGRAL FLUX (/day·cm^2)	SATURATION CROSS-SECTION (cm^2)	EVENT RATE (/DAY)	EVENT RATE (FIT)	MTBE (YEARS)
LEO (ISS)	45	5.5×10^{-4}	8.14×10^{-5}	4.48×10^{-8}	1.87	6.11×10^{4}
GEO		1.8×10^{-3}		1.49×10^{-7}	6.22	1.83×10^{4}

Table 29. SET Event Rate Calculations for Worst-Case LEO and GEO Orbits at VIN = 1.8 V, VOUT = 1.2 V, Load = 0.5 A, and SET ≥ |5|% from the Nominal Output Voltage

ORBIT TYPE	ONSET LET_{EFF} ($MeV \cdot cm^2/mg$)	CREME96 INTEGRAL FLUX (/day·cm^2)	SATURATION CROSS-SECTION (cm^2)	EVENT RATE (/DAY)	EVENT RATE (FIT)	MTBE (YEARS)
LEO (ISS)	50	3.92×10^{-4}	1.11×10^{-5}	4.36×10^{-9}	0.181	6.28×10^{5}
GEO		1.3×10^{-3}		1.41×10^{-8}	0.59	1.93×10^{5}

Table 30. SET Event Rate Calculations for Worst-Case LEO and GEO Orbits at VIN = 1.8 V, VOUT = 1.2 V, Load = 3 A, and SET ≥ |10| % from the Nominal Output Voltage

ORBIT TYPE	ONSET LET_{EFF} ($MeV \cdot cm^2/mg$)	CREME96 INTEGRAL FLUX (/day·cm^2)	SATURATION CROSS-SECTION (cm^2)	EVENT RATE (/DAY)	EVENT RATE (FIT)	MTBE (YEARS)
LEO (ISS)	45	5.5×10^{-4}	6.05×10^{-5}	3.33×10^{-8}	1.39	8.22×10^{4}
GEO		1.8×10^{-3}		1.1×10^{-7}	4.62	2.47×10^{4}

Table 31. SET Event Rate Calculations for Worst-Case LEO and GEO Orbits at VIN = 1.8 V, VOUT = 1.2 V, Load = 0.5 A, and SET ≥ |10| % from the Nominal Output Voltage

ORBIT TYPE	ONSET LET_{EFF} ($MeV \cdot cm^2/mg$)	CREME96 INTEGRAL FLUX (/day·cm^2)	SATURATION CROSS-SECTION (cm^2)	EVENT RATE (/DAY)	EVENT RATE (FIT)	MTBE (YEARS)
LEO (ISS)	45	5.5×10^{-4}	3.99×10^{-6}	2.19×10^{-9}	0.092	1.25×10^{6}
GEO		1.8×10^{-3}		7.32×10^{-9}	0.305	3.74×10^{5}

Table 32. SET Event Rate Calculations for Worst-Case LEO and GEO Orbits at VIN = 1.8 V, VOUT = 1.2 V, Load = 3 A, and Positive Polarity

ORBIT TYPE	ONSET LET_{EFF} ($MeV \cdot cm^2/mg$)	CREME96 INTEGRAL FLUX (/day·cm^2)	SATURATION CROSS-SECTION (cm^2)	EVENT RATE (/DAY)	EVENT RATE (FIT)	MTBE (YEARS)
LEO (ISS)	54	2.94×10^{-4}	3.12×10^{-5}	9.16×10^{-9}	0.3816	2.99×10^{5}
GEO		9.32×10^{-4}		2.91×10^{-8}	1.211	9.43×10^{4}

Table 33. SET Event Rate Calculations for Worst-Case LEO and GEO Orbits at VIN = 1.8 V, VOUT = 1.2 V, Load = 3 A, and Negative Polarity

ORBIT TYPE	ONSET LET_{EFF} ($MeV \cdot cm^2/mg$)	CREME96 INTEGRAL FLUX (/day·cm^2)	SATURATION CROSS-SECTION (cm^2)	EVENT RATE (/DAY)	EVENT RATE (FIT)	MTBE (YEARS)
LEO (ISS)	40	8.41×10^{-4}	2.77×10^{-4}	2.33×10^{-7}	9.71	1.18×10^{4}
GEO		3×10^{-3}		8.31×10^{-7}	34.61	3.29×10^{3}

Table 34. SET Event Rate Calculations for Worst-Case LEO and GEO Orbits at VIN = 1.8 V, VOUT = 1.2 V, Load = 0.5 A, and Positive Polarity

ORBIT TYPE	ONSET LET$_{EFF}$ (MeV·cm^2/mg)	CREME96 INTEGRAL FLUX (/day·cm^2)	SATURATION CROSS-SECTION (cm^2)	EVENT RATE (/DAY)	EVENT RATE (FIT)	MTBE (YEARS)
LEO (ISS)	58	2.02×10^{-4}	2.11×10^{-5}	4.27×10^{-9}	0.178	6.42×10^{5}
GEO		6.14×10^{-4}		1.29×10^{-8}	0.539	2.11×10^{5}

Table 35. SET Event Rate Calculations for Worst-Case LEO and GEO Orbits at VIN = 1.8 V, VOUT = 1.2 V, Load = 0.5 A, and Negative Polarity

ORBIT TYPE	ONSET LET$_{EFF}$ (MeV·cm^2/mg)	CREME96 INTEGRAL FLUX (/day·cm^2)	SATURATION CROSS-SECTION (cm^2)	EVENT RATE (/DAY)	EVENT RATE (FIT)	MTBE (YEARS)
LEO (ISS)	54	2.94×10^{-4}	7.78×10^{-6}	2.28×10^{-9}	0.095	1.2×10^{6}
GEO		9.32×10^{-4}		7.25×10^{-9}	0.302	3.78×10^{5}

Table 36. Soft-Start SET Event Rate Calculations for Worst-Case LEO and GEO Orbits

ORBIT TYPE	ONSET LET$_{EFF}$ (MeV·cm^2/mg)	CREME96 INTEGRAL FLUX (/day·cm^2)	SATURATION CROSS-SECTION (cm^2)	EVENT RATE (/DAY)	EVENT RATE (FIT)	MTBE (YEARS)
LEO (ISS)	85	2.43×10^{-5}	1.09×10^{-6}	2.65×10^{-11}	1.1×10^{-3}	1.03×10^{8}
GEO		6.81×10^{-5}		7.42×10^{-11}	3.1×10^{-3}	3.69×10^{7}

Table 37. Power Good (PG) SET Event Rate Calculations for Worst-Case LEO and GEO Orbits

ORBIT TYPE	ONSET LET$_{EFF}$ (MeV·cm^2/mg)	CREME96 INTEGRAL FLUX (/day·cm^2)	SATURATION CROSS-SECTION (cm^2)	EVENT RATE (/day)	EVENT RATE (FIT)	MTBE (YEARS)
LEO (ISS)	85	2.43×10^{-5}	2.36×10^{-7}	5.74×10^{-12}	2.39×10^{-4}	4.76×10^{8}
GEO		6.81×10^{-5}		1.6×10^{-11}	6.7×10^{-4}	1.7×10^{8}

10 Summary

The purpose of this report is to summarize the TPS7H1101A-SP SEE performance under heavy-ions irradiation. The data shows the device is SEL-, SEB/SEGR-, and SET-free for deviations higher than ±5% from the nominal output voltage at V_{IN} = 5 V, V_{OUT} = 2.5 V, and load of three Amps across the full electrical specifications. SETs for V_{IN} = 5 V, V_{OUT} = 2.5 V at 0.5, and three Amps ≥ 3%, 4%, and 5% from the output nominal voltage are presented and discussed. Also, for V_{IN} = 1.8 V, V_{OUT} = 1.2 V at 0.5 and three Amps for ≥ 5% from the output nominal voltage. Weibull fit was created when applicable and LEO (ISS) and GEO orbit rate calculations were calculated and presented. The worst case on orbit rate MTBE (mean-time between events) is shown to be on the order of 10^4 years.

Total Ionizing Dose From SEE Experiments

The TPS7H1101A-SP is rated for a total ionizing dose (TID) of 100 krad (Si). In the course of the SEE testing, the heavy-ion exposure delivered approximately 10 krad (Si) per 10^7 ions/cm^2 and approximately 1 krad (Si) per 10^6 ions/cm^2 run. The cumulative TID exposure for all five units was controlled to be below the 100 krad(Si).

Orbital Environment Estimations

To calculate on-orbit SEE event rates, you need both the device SEE cross section and the flux of particles encountered in a particular orbit. Device SEE cross sections are usually determined experimentally while flux of particles in orbit is calculated using various codes. For the purpose of generating some event rates, a Low-Earth Orbit (LEO) and a Geostationary-Earth Orbit (GEO) were calculated using CREME96. CREME96 code, short for Cosmic Ray Effects on Micro-Electronics, is a suite of programs that enable estimation of the radiation environment in near-Earth orbits [10, 11]. CREME96 is one of several tools available in the aerospace industry to provide accurate space environment calculations. Over the years since its introduction, the CREME models have been compared with on-orbit data and demonstrated their accuracy. In particular, CREME96 incorporates realistic “worst-case” solar particle event models where fluxes can increase by several orders-of-magnitude over short periods of time.

For the purposes of generating conservative event rates, the worst-week model (based on the biggest solar event lasting a week in the last 45 years) was selected, which has been equated to a 99%-confidence level worst-case event [12, 13]. The integrated flux includes protons to heavy ions from solar and galactic sources. A minimal shielding configuration is assumed at 100 mils (2.54 mm) of aluminum. Two orbital environments were estimated: that of the International Space Station (ISS), which is LEO and the GEO environment. Figure 33 shows the integrated flux (from high LET to low) for these two environments.

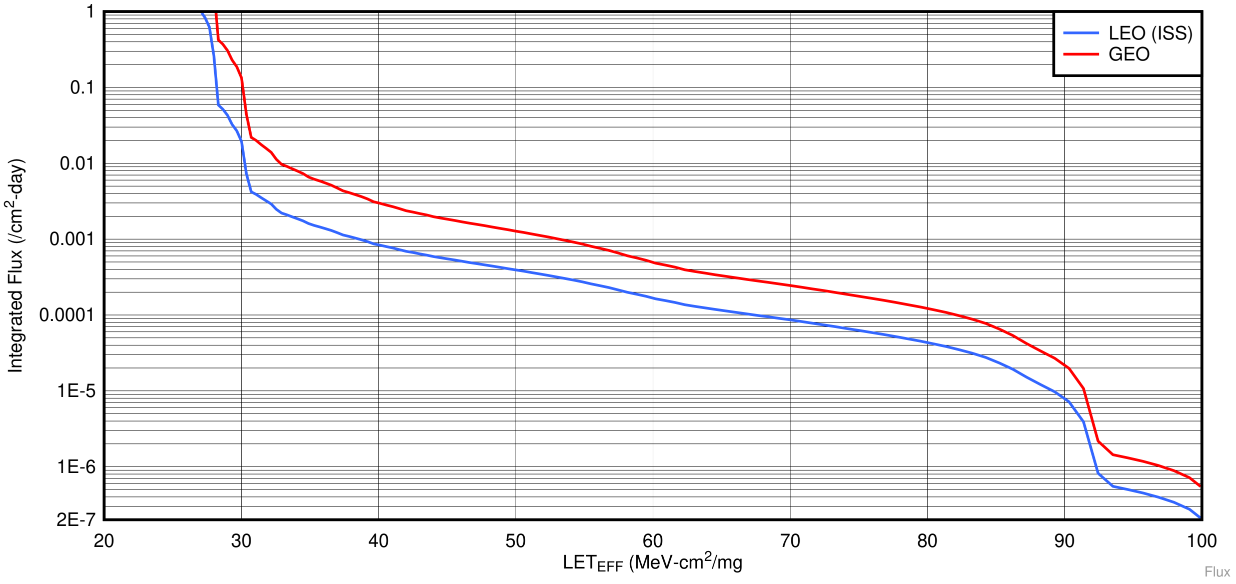

Note that the y-axis represents flux integrated from higher LET to lower LET. The value of integral flux at any specific LET value is actually the integral of all ion events at that specific LET value to all higher LETs.

Figure 33. Integral Particle Flux Versus LETEFF for a LEO-ISS (blue curve) and a GEO (red curve) Environment as Calculated by CREME96 Assuming Worst-week and 100 mils (2.54 mm) of Aluminum Shielding

Figure 33 shows the Integral Particle Flux versus LET$_{EFF}$ for an LEO-ISS (blue curve) and a GEO (red curve) environment as calculated by CREME96 assuming worst-week and 100 mils (2.54 mm) of aluminum shielding. Note that the y-axis represents flux integrated from higher LET to lower LET. The value of integral flux at any specific LET value is actually the integral of all ion events at that specific LET value to all higher LETs.

Using this data, you can extract integral particle fluxes for any arbitrary LET of interest. To simplify the calculation of event rates, assume that all cross section curves are square, meaning that below the onset LET, the cross section is identically zero while above the onset LET, the cross section is uniformly equal to the saturation cross section. Figure 34 illustrates the approximation with the green curve being the actual Weibull fit to the data with the “square” approximation shown as the red-dashed line. This allows you to calculate event rates with a single multiplication, the event rate becoming simply the product of the integral flux at the onset LET, and the saturation cross section. Obviously, this leads to an over-estimation of the event rate since the area under the square approximation is larger than the actual cross section curve, but for the purposes of calculating upper-bound event rate estimates, this modification avoids the need to do the integral over the flux and cross section curves.

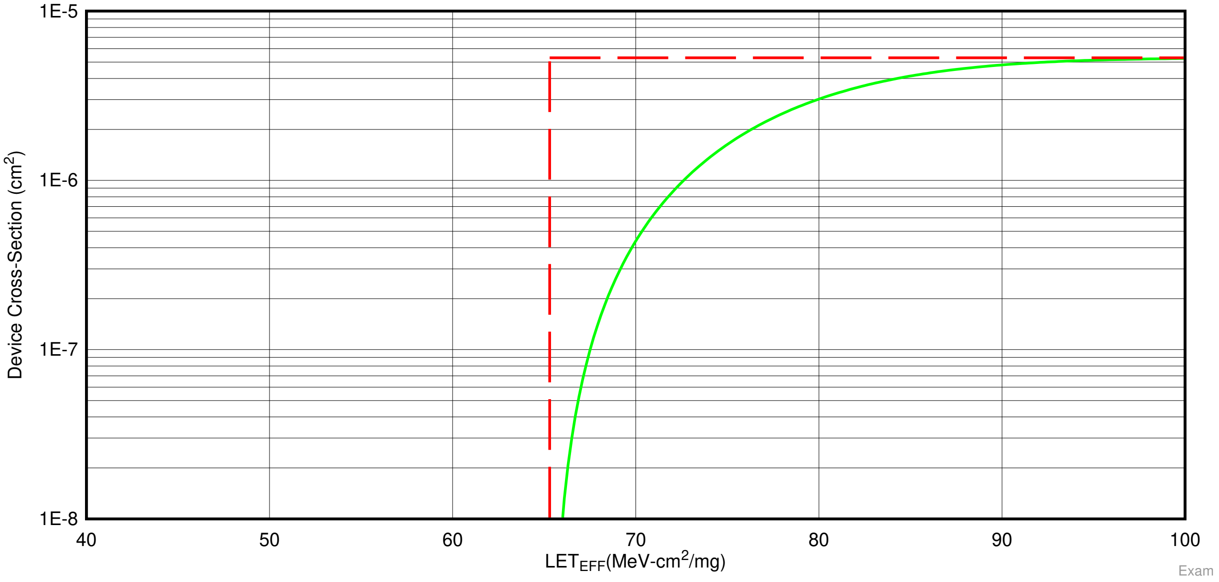

Figure 34. Device Cross section Versus LET$_{EFF}$ Showing How the Weibull Fit (Green) is “Simplified” with the Use a Square Approximation (Red Dashed Line)

Figure 34 shows a device cross section versus LET$_{EFF}$, showing how the Weibull fit (green) is “simplified” with the use a square approximation (red dashed line).

To demonstrate how the event rates in this report were calculated, assume that you wish to calculate an event rate for a GEO orbit for the device whose cross section is shown in Figure 34. Using the red curve in Figure 33 and the onset LET value obtained from Figure 34 (approximately 65 MeV-cm2/mg), you find the GEO integral flux to be approximately 3.24 × 10^{-4} ions/cm^2-day. The event rate is the product of the integral flux and the saturation cross section in Figure 34 (approximately 5.3 x 10^{-6} cm^2):

$$GEO\ Event\ Rate = \left(3.24 \times 10^{-4} \frac{ions}{cm^2 \times day}\right) \times (5.3 \times 10^{-6}\ cm^2) = 1.71 \times 10^{-9}\ \frac{events}{day} \tag{5}$$

$$GEO\ Event\ Rate = 0.71 \times 10^{-10} \frac{events}{hr} = 0.071\ FIT \tag{6}$$

$$MTBF = 1{,}607{,}820\ Years \tag{7}$$

Appendix C

Confidence Interval Calculations

For conventional products where hundreds of failures are seen during a single exposure, you can determine the average failure rate of parts being tested in a heavy-ion beam as a function of fluence with a high degree of certainty and reasonably tight standard deviation. This means that you have a good deal of confidence that the calculated cross section is accurate.

With radiation-hardened parts however, determining the cross section becomes more difficult since often few, or even, no failures are observed during an entire exposure. Determining the cross section using an average failure rate with standard deviation is no longer a viable option, and the common practice of assuming a single error occurred at the conclusion of a null-result can end up in a greatly underestimated cross section.

In cases where observed failures are rare or non-existent, the use of confidence intervals and the Chi-Squared distribution is indicated. The Chi-Squared distribution is particularly well-suited for the determining a reliability level when the failures occur at a constant rate. In the case of SEE testing where the ion events are random in time and position within the irradiation area, you expect a failure rate that is independent of time (presuming that parametric shifts induced by the total ionizing dose do not affect the failure rate), so the use of Chi-Squared statistical techniques is valid (since events are rare an exponential or Poisson distribution is usually used).

In a typical SEE experiment, the device-under-test (DUT) is exposed to a known, fixed fluence (ions/cm^2) while the DUT is monitored for failures. This is analogous to fixed-time reliability testing and, more specifically, time-terminated testing, where the reliability test is terminated after a fixed amount of time whether or not a failure has occurred (in the case of SEE tests fluence is substituted for time and hence it is a fixed fluence test) [14]. Calculating a confidence interval specifically provides a range of values which is likely to contain the parameter of interest (the actual number of failures/fluence). Confidence intervals are constructed at a specific confidence level. For example, a 95% confidence level implies that if a given number of units was sampled numerous times and a confidence interval was estimated for each test, the resulting set of confidence intervals would bracket the true population parameter in about 95% of the cases.

To estimate the cross section from a null-result (no fails observed for a given fluence) with a confidence interval, start with the standard reliability determination of lower-bound (minimum) mean-time-to-failure for fixed-time testing (an exponential distribution is assumed):

$$\mathrm{MTTF} = \frac{2nT}{\chi^2_{2(d+1);100\left(1-\frac{\alpha}{2}\right)}}$$

where

- *MTTF* is the minimum (lower-bound) mean-time-to-failure
- *n* is the number of units tested (presuming each unit is tested under identical conditions)
- *T* is the test time
- x^2 is the chi-square distribution evaluated at 100(1 – α / 2) confidence level
- d is the degrees-of-freedom (the number of failures observed) (8)

With slight modification for this purpose, invert the inequality and substitute *F* (fluence) in the place of *T*:

$$\text{MFTF} = \frac{2nF}{\chi^2_{2(d+1);100\left(1-\frac{\alpha}{2}\right)}}$$

where

- *MFTF* is mean-fluence-to-failure
- *F* is the test fluence
- x^2 is the chi-square distribution evaluated at 100(1 – α / 2) confidence
- *d* is the degrees-of-freedom (the number of failures observed) (9)

The inverse relation between MTTF and failure rate is mirrored with the MFTF. Thus the upper-bound cross section is obtained by inverting the MFTF:

$$\sigma = \frac{\chi^2_{2(d+1);100\left(1-\frac{\alpha}{2}\right)}}{2nF} \quad (10)$$

Assume that all tests are terminated at a total fluence of 10^6 ions/cm^2. Also assume that you have a number of devices with very different performances that are tested under identical conditions. Assume a 95% confidence level (σ = 0.05). Note that as *d* increases from zero events to 100 events, the actual confidence interval becomes smaller, indicating that the range of values of the true value of the population parameter (in this case, the cross section) is approaching the mean value + 1 standard deviation. This makes sense when you consider that as more events are observed, the statistics are improved such that uncertainty in the actual device performance is reduced.

Table 38. Experimental Example Calculation of Mean-Fluence-to-Failure (MFTF) and, σ Using a 95% Confidence Interval[1]

DEGREES-OF-FREEDOM (d)	2(d + 1)	χ^2 @ 95%	CALCULATED CROSS SECTION (cm^2)		
			UPPER-BOUND @ 95% CONFIDENCE	MEAN	AVERAGE + STANDARD DEVIATION
0	2	7.38	3.69E–06	0.00E+00	0.00E+00
1	4	11.14	5.57E–06	1.00E–06	2.00E–06
2	6	14.45	7.22E–06	2.00E–06	3.41E–06
3	8	17.53	8.77E–06	3.00E–06	4.73E–06
4	10	20.48	1.02E–05	4.00E–06	6.00E–06
5	12	23.34	1.17E–05	5.00E–06	7.24E–06
10	22	36.78	1.84E–05	1.00E–05	1.32E–05
50	102	131.84	6.59E–05	5.00E–05	5.71E–05
100	202	243.25	1.22E–04	1.00E–04	1.10E–04

(1) Using a 95% confidence for several different observed results (d = 0, 1, 2...100 observed events during fixed-fluence tests) assuming 10^6 ion/cm^2 for each test.

Appendix D

SLVK045–February 2020

References

1. M. Shoga and D. Binder, “Theory of Single Event Latchup in Complementary Metal-Oxide Semiconductor Integrated Circuits”, IEEE Trans. Nucl. Sci, Vol. 33(6), Dec. 1986, pp. 1714-1717.
2. G. Bruguier and J.M. Palau, “Single particle-induced latchup”, IEEE Trans. Nucl. Sci, Vol. 43(2), Mar. 1996, pp. 522-532.
3. G. H. Johnson, J. H. Hohl, R. D. Schrimpf and K. F. Galloway, "Simulating single-event burnout of n-channel power MOSFET's," in IEEE Transactions on Electron Devices, vol. 40, no. 5, pp. 1001-1008, May 1993.
4. J. R. Brews, M. Allenspach, R. D. Schrimpf, K. F. Galloway, J. L. Titus and C. F. Wheatley, "A conceptual model of a single-event gate-rupture in power MOSFETs," in IEEE Transactions on Nuclear Science, vol. 40, no. 6, pp. 1959-1966, Dec. 1993.
5. G. H. Johnson, R. D. Schrimpf, K. F. Galloway, and R. Koga, “Temperature dependence of singleevent burnout in n-channel power MOSFETs [for space application],” IEEE Trans. Nucl. Sci., 39(6), Dec. 1992, pp. 1605-1612.
6. TAMU Radiation Effects Facility
7. “The Stopping and Range of Ions in Matter” (SRIM) software simulation tools website. http://www.srim.org/index.htm#SRIMMENU
8. https://creme.isde.vanderbilt.edu/CREME-MC
9. A. J. Tylka, et al., "CREME96: A Revision of the Cosmic Ray Effects on Micro-Electronics Code", IEEE Trans. Nucl. Sci., 44(6), 1997, pp. 2150-2160.
10. A. J. Tylka, W. F. Dietrich, and P. R. Bobery, “Probability distributions of high-energy solar-heavy-ion fluxes from IMP-8: 1973-1996”, IEEE Trans. on Nucl. Sci., 44(6), Dec. 1997, pp. 2140 – 2149.
11. A. J. Tylka, J. H. Adams, P. R. Boberg, et al.,“CREME96: A Revision of the Cosmic Ray Effects on Micro-Electronics Code”, Trans. on Nucl. Sci, 44(6), Dec. 1997, pp. 2150 – 2160.
12. D. Kececioglu, “Reliability and Life Testing Handbook”, Vol. 1, PTR Prentice Hall, New Jersey,1993, pp. 186-193.

IMPORTANT NOTICE AND DISCLAIMER

TI PROVIDES TECHNICAL AND RELIABILITY DATA (INCLUDING DATA SHEETS), DESIGN RESOURCES (INCLUDING REFERENCE DESIGNS), APPLICATION OR OTHER DESIGN ADVICE, WEB TOOLS, SAFETY INFORMATION, AND OTHER RESOURCES “AS IS” AND WITH ALL FAULTS, AND DISCLAIMS ALL WARRANTIES, EXPRESS AND IMPLIED, INCLUDING WITHOUT LIMITATION ANY IMPLIED WARRANTIES OF MERCHANTABILITY, FITNESS FOR A PARTICULAR PURPOSE OR NON-INFRINGEMENT OF THIRD PARTY INTELLECTUAL PROPERTY RIGHTS.

These resources are intended for skilled developers designing with TI products. You are solely responsible for (1) selecting the appropriate TI products for your application, (2) designing, validating and testing your application, and (3) ensuring your application meets applicable standards, and any other safety, security, regulatory or other requirements.

These resources are subject to change without notice. TI grants you permission to use these resources only for development of an application that uses the TI products described in the resource. Other reproduction and display of these resources is prohibited. No license is granted to any other TI intellectual property right or to any third party intellectual property right. TI disclaims responsibility for, and you will fully indemnify TI and its representatives against, any claims, damages, costs, losses, and liabilities arising out of your use of these resources.

TI’s products are provided subject to TI’s Terms of Sale or other applicable terms available either on ti.com or provided in conjunction with such TI products. TI’s provision of these resources does not expand or otherwise alter TI’s applicable warranties or warranty disclaimers for TI products.

TI objects to and rejects any additional or different terms you may have proposed.

Mailing Address: Texas Instruments, Post Office Box 655303, Dallas, Texas 75265
Copyright © 2022, Texas Instruments Incorporated